Advanced Review

Resonance energy flow dynamics of coherently delocalized excitons in biological and macromolecular systems: Recent theoretical advances and open issues

Seogjoo Jang[1]* and Yuan-Chung Cheng[2]

Recent experimental and theoretical studies suggest that biological photosynthetic complexes utilize the quantum coherence in a positive manner for efficient and robust flow of electronic excitation energy. Clear and quantitative understanding of such suggestion is important for identifying the design principles behind efficient flow of excitons coherently delocalized over multiple chromophores in condensed environments. Adaptation of such principles for synthetic macromolecular systems has also significant implication for the development of novel photovoltaic systems. Advanced theories of resonance energy transfer are presented, which can address these issues. Applications to photosynthetic light harvesting complex systems and organic materials demonstrate the capabilities of new theoretical approaches and future challenges. © 2012 John Wiley & Sons, Ltd.

How to cite this article:
WIREs Comput Mol Sci 2012, 00: 1–21 doi: 10.1002/wcms.1111

INTRODUCTION

In molecular crystals,[1–6] biological photosynthetic complexes,[7–10] and aggregates of organic chromophores,[11–18] excitons provide practical means to understand the energetics and the dynamics of collective electronic processes that go beyond one molecular unit. A common form of excitons found in these systems is so-called Frenkel exciton,[1,19] which can be defined in the direct product space of individual molecular excitations. Here, single exciton refers to the coherent superposition of states where only one molecule is excited while others are in the ground electronic state, double exciton refers to the one formed by the states with only two molecules excited, and so on. Thus, the excitation of each molecule corresponds to the limit of single exciton fully localized at one molecule.

Because of exchange and Coulomb interactions, excitons are easily delocalized among different molecules with varying degrees of time and length scales. The manner of such delocalization reflects the relative arrangement, dynamics, and energetics of molecules at nanometer length scale. Thus, the frequency and time domain properties of excitons may serve as sensitive probes of such structural and dynamical information, and vice versa. With the advances in selectivity and time resolution of spectroscopic techniques, steady advances have been made in real-time description of exciton dynamics at different timescales and environments.

At the simplest level, the dynamics of exciton (excitation) between two weakly coupled molecules can be described as a Fermi golden rule (FGR) rate process. Förster's theory,[20] the earliest and the most successful theory, is an application of the FGR between two localized excitons with transition dipole coupling. This was soon followed by Dexter's extension[21] for multipolar and exchange interactions.

*Correspondence to: seogjoo.jang@qc.cuny.edu

[1]Department of Chemistry and Biochemistry, Queens College of the City University of New York, NY, USA

[2]Department of Chemistry and Center for Quantum Science and Engineering, National Taiwan University, Taipei City, Taiwan

DOI: 10.1002/wcms.1111

 © 2012 John Wiley & Sons, Ltd.

In practice, Förster's or Dexter's theory can be applied to more than two molecular excitations as long as the electronic couplings are so small that the excitons are virtually localized at each molecule. This is the case for the so-called host–guest systems where low concentration of chromophores (guest molecules) is embedded in the media of optically inactive host molecules. The dynamics of exciton can be described in terms of hopping processes, with each rate given by the Förster's or Dexter's theory. Owing to the disorder in the distribution of the guest molecules, the global dynamics of exciton even in this limit poses challenging problems. Great amount of theoretical and experimental efforts were made to address these issues.[22–29]

In the other limit of strong electronic coupling between two molecules, excitons are fully delocalized. Traditionally, these systems were studied by frequency domain spectroscopy where clear signature of exciton formation can be seen. For larger aggregates such as molecular crystals or self-assemblies, the band theory can describe major features of spectral lineshapes and the exciton dynamics. In practice, because of the disorder and the electron–phonon coupling, excitons have finite coherence lengths and the band theory breaks down at some level. Grover and Silbey[30] developed a unified formal framework applicable to such general situation. In this theory, the exciton diffusion constant can be expressed as the sum of hopping and band contributions. An alternative approach of generalized master equation formalism was also developed by Kenkre and Knox.[31]

With the discovery of intricate structures of photosynthetic light harvesting complexes[10,32] and the progress in the capability to synthesize new macromolecules or nanometer-scale assemblies, it has become an important issue to understand the dynamics of excitons among tens or hundreds of chromophores arranged in a nontrivial manner.[13,33–39] If the couplings between chromophores are weak, the dynamics of exciton can be described by rate processes as in the case of porphyrin arrays.[40] However, in general, excitons are delocalized and their behavior depends sensitively on electronic couplings, electron–phonon interactions, and the disorder. The exciton dynamics in these systems are complex and may not be fully specified by simple rate or transport coefficients.

Despite the complexity, theoretical studies suggest that photosynthetic light harvesting complexes utilize the delicate nature of excitons for efficient and robust collection/transfer of excitons.[41–44] Whether such utilization is possible in synthetic systems is a question that has great implications for solar energy conversion,[45,46] optical sensor development, and imaging. For clear understanding of the design principles, detailed spatio-temporal information on excitons related to certain optoelectronic functionality is needed. Single molecule spectroscopy[47,48] and nonlinear spectroscopy can provide much more information than linear ensemble spectroscopy in this regard.[49–52] In particular, recent two-dimensional electronic spectroscopy (2DES) experiments observed coherent beating of third-order response functions in photosynthetic complexes[53–56] and conjugated polymers,[16] which have been attributed as evidences for excitonic quantum coherence. These discoveries motivated new or renewed theoretical and computational studies,[57–61] which by themselves have generated intriguing conceptual and theoretical issues.

The objective of this review is to expose some theoretical issues to be resolved for quantitative understanding of the resonance energy transfer (RET) dynamics involving coherently delocalized excitons as in macromolecules or nanoscale assemblies. A few theoretical advances have already been made to this end, but much more are needed and expected. While comprehensive and objective review of all recent works is highly desirable, it goes beyond the scope of present review. Rather, we here focus mainly on our theories and computational studies, and refer to other works when relevant.

REVIEW OF FÖRSTER'S RESONANCE ENERGY TRANSFER

The theory of Förster's resonance energy transfer (FRET)[20] has had profound impact in all the fields of chemistry, physics, and biology involving luminescence properties.[62–65] While recent progress in experimental[66,67] and computational techniques[15,68–70] opened up ways to probe the energy transfer process directly, Förster's theory still enjoys a critical role in modeling and understanding experimental results.[13,38,39,71–81] Another important application of Förster's theory is for the determination of nanometer-scale distances through detection of fluorescence signals. This is now a well-established biophysical technique and is also referred to as FRET[66,67,82–87] (fluorescence resonance energy transfer[a]), which is not the major subject of the present work.

Although Förster's theory was reviewed by himself[2] and other experts,[62,64] a derivation of Förster's spectral overlap expression employing modern terminology is not easily available. Such a derivation is contained in a recent work,[88] which is briefly reviewed below.

 © 2012 John Wiley & Sons, Ltd.

Consider the following transfer of exciton from D^* to A:

$$D^* + A \rightarrow D + A^*, \tag{1}$$

where D^* (D) is the excited (ground) state donor and A (A^*) is the ground (excited) state acceptor. The ground electronic state consisting of D and A is denoted as $|g\rangle$, the donor exciton state consisting of D^* and A as $|D\rangle$, and the acceptor exciton state consisting of D and A^* as $|A\rangle$. All other degrees of freedom are defined as the bath. The bath Hamiltonian corresponding to $|g\rangle$ is H_b.

Let us assume that an impulsive and selective creation of $|D\rangle$ is possible while the bath remains in the canonical ensemble for $|g\rangle$. The corresponding initial condition of the total density operator $\rho(t)$ is

$$\rho(0) = |D\rangle\langle D|\mathrm{e}^{-\beta H_b}/Z_b, \tag{2}$$

where $\beta = 1/k_B T$ and $Z_b = Tr_b\{\mathrm{e}^{-\beta H_b}\}$. Neglecting the spontaneous decay and assuming that the exciton stays in the excited space spanned by $|D\rangle$ and $|A\rangle$ long enough, the effective total Hamiltonian governing the exciton and bath can be expressed as

$$\begin{aligned} H = &(E_D + B_D)|D\rangle\langle D| + (E_A + B_A)|A\rangle\langle A| \\ &+ J(|D\rangle\langle A| + |A\rangle\langle D|) + H_b, \end{aligned} \tag{3}$$

where E_D is the energy of $|D\rangle$, E_A is the energy of $|A\rangle$, and J is the electronic coupling. B_D is a bath operator representing the displacement of bath modes upon the creation of $|D\rangle$ and B_A is that for $|A\rangle$. Note that off-diagonal coupling to the bath is ignored in the model.

At time $t > 0$, the probability to find the exciton state $|A\rangle$ is

$$P_A(t) = Tr_b\left\{\langle A|\mathrm{e}^{-iHt/\hbar}\rho(0)\,\mathrm{e}^{iHt/\hbar}|A\rangle\right\}. \tag{4}$$

For short enough time compared to $\hbar/J$, a perturbation expansion of the above expression with respect to $H_{DA} = J(|D\rangle\langle A| + |A\rangle\langle D|)$ can be made. Expanding $P_A(t)$ up to the second order of t and taking its time derivative, we obtain the following time dependent rate of energy transfer:

$$\begin{aligned} k(t) = \frac{2J^2}{\hbar^2}\mathrm{Re}\Bigg[\int_0^t \mathrm{d}\,t' e^{i(E_D - E_A)t'/\hbar} \\ \times \frac{1}{Z_b} Tr_b\left\{\mathrm{e}^{i(H_b + B_D)t/\hbar}\,\mathrm{e}^{-i(H_b + B_A)t'/\hbar}\right. \\ \left.\times\,\mathrm{e}^{-i(H_b + B_D)(t-t')/\hbar}\,\mathrm{e}^{-\beta H_b}\right\}\Bigg]. \end{aligned} \tag{5}$$

Assume that the bath Hamiltonian is an independent sum of donor and acceptor baths as follows:

$$H_b = H_{b_D} + H_{b_A}. \tag{6}$$

Then $\mathrm{e}^{-\beta H_b}/Z_b = \rho^g_{b_D}\rho^g_{b_A}$, where $\rho^g_{b_D} = \mathrm{e}^{-\beta H_{b_D}}/Z_{b_D}$ and $\rho^g_{b_A} = \mathrm{e}^{-\beta H_{b_A}}/Z_{b_A}$ with $Z_{b_D} = Tr_{b_D}\{\mathrm{e}^{-\beta H_{b_D}}\}$ and $Z_{b_A} = Tr_{b_A}\{\mathrm{e}^{-\beta H_{b_A}}\}$. In addition, let us assume that B_D commutes with H_{b_A} and that B_A commutes with H_{b_D}. Then, the trace over the bath in Eq. (5) can be decoupled into those for the donor and the acceptor baths as follows:

$$\begin{aligned} k(t) = \frac{2J^2}{\hbar^2}\mathrm{Re}\Bigg[\int_0^t \mathrm{d}\,t'\,\mathrm{e}^{i(E_D - E_A)t'/\hbar} \\ \times \frac{1}{Z_{b_A}} Tr_{b_A}\left\{\mathrm{e}^{iH_{b_A}t/\hbar}\,\mathrm{e}^{-i(H_{b_A} + B_A)t'/\hbar}\right. \\ \left.\times\,\mathrm{e}^{-iH_{bA}(t-t')/\hbar}\,\mathrm{e}^{-\beta H_{b_A}}\right\} \\ \times \frac{1}{Z_{b_D}} Tr_{b_D}\left\{\mathrm{e}^{i(H_{b_D} + B_D)t/\hbar}\,\mathrm{e}^{-iH_{b_D}t'/\hbar}\right. \\ \left.\times\,\mathrm{e}^{-i(H_{b_D} + B_D)(t-t')/\hbar}\,\mathrm{e}^{-\beta H_{b_D}}\right\}\Bigg]. \end{aligned} \tag{7}$$

If the bath becomes equilibrated with the excited donor before the transfer of excitation occurs, the following approximation can be made:

$$\begin{aligned} \mathrm{e}^{-i(H_{b_D} + B_D)(t-t')/\hbar}\rho^g_{b_D}\,\mathrm{e}^{i(H_{b_D} + B_D)(t-t')/\hbar} \\ \approx \frac{\mathrm{e}^{-\beta(H_{b_D} + B_D)}}{Z'_{b_D}} \equiv \rho^e_{b_D}, \end{aligned} \tag{8}$$

where $Z'_{b_D} = Tr_{b_D}\{\mathrm{e}^{-\beta(H_{b_D} + B_D)}\}$. Inserting the above approximation into Eq. (7) and going to the limit of $t = \infty$, we obtain the following FGR expression:

$$\begin{aligned} k_F = \frac{2J^2}{\hbar^2}\mathrm{Re}\Bigg[\int_0^\infty \mathrm{d}\,t'\,\mathrm{e}^{i(\epsilon_D - \epsilon_A)t'/\hbar} \\ \times \frac{1}{Z_{bA}} Tr_{bA}\left\{\mathrm{e}^{iH_{bA}t'/\hbar}\,\mathrm{e}^{-i(H_{bA} + B_A)t'/\hbar}\,\mathrm{e}^{-\beta H_{bA}}\right\} \\ \times \frac{1}{Z'_{bD}} Tr_{bD}\left\{\mathrm{e}^{i(H_{bD} + B_D)t'/\hbar}\,\mathrm{e}^{-iH_{bD}t'/\hbar}\,\mathrm{e}^{-\beta(H_{bD} + B_D)}\right\}\Bigg] \end{aligned} \tag{9}$$

This can be expressed in the frequency domain in terms of the following lineshape functions of the donor emission and acceptor absorption:

$$\begin{aligned} L_D(\omega) = \int_{-\infty}^{\infty} \mathrm{d}\,t\;\mathrm{e}^{-i\omega t + i\epsilon_D t/\hbar} \\ \times \frac{1}{Z'_{bD}} Tr_{bD}\left\{\mathrm{e}^{i(H_{bD} + B_D)t/\hbar}\,\mathrm{e}^{-iH_{bD}t/\hbar}\,\mathrm{e}^{-\beta(H_{bD} + B_D)}\right\}, \end{aligned} \tag{10}$$

$$\begin{aligned} I_A(\omega) = \int_{-\infty}^{\infty} \mathrm{d}\,t\;\mathrm{e}^{i\omega t - i\epsilon_A t/\hbar} \\ \times \frac{1}{Z_{bA}} Tr_{bA}\left\{\mathrm{e}^{iH_{bA}t/\hbar}\,\mathrm{e}^{-i(H_{bA} + B_A)t/\hbar}\,\mathrm{e}^{-\beta H_{bA}}\right\}. \end{aligned} \tag{11}$$

 © 2012 John Wiley & Sons, Ltd.

Inserting inverse Fourier transforms of the above equations into Eq. (9), we obtain

$$k_F = \frac{J^2}{2\pi\hbar^2}\int_{-\infty}^{\infty} \mathrm{d}\,\omega L_D(\omega) I_A(\omega). \tag{12}$$

Equation (12) is equivalent to Förster's spectral overlap expression as will be shown below. First, the integration over ω in Eq. (12) can be converted into that over $\tilde{\nu} = \omega/(2\pi c)$ as follows:

$$k_F = \frac{c}{\hbar^2} J^2 \int_{-\infty}^{\infty} \mathrm{d}\,\tilde{\nu} L_D(2\pi c\tilde{\nu}) I_A(2\pi c\tilde{\nu}). \tag{13}$$

Employing the standard theory of emission and absorption, $L_D(\omega)$ can be expressed in terms of the normalized emission lineshape $f_D(\tilde{\nu})$, and $I_A(\omega)$ in terms of the molar extinction coefficient $\epsilon_A(\tilde{\nu})$. As detailed in the Appendix of Ref 88, one can establish the following identities:

$$f_D(\tilde{\nu}) = \frac{\tilde{\nu}^3 L_D(2\pi c\tilde{\nu})}{\int \mathrm{d}\,\tilde{\nu}\tilde{\nu}^3 L_D(2\pi c\tilde{\nu})} = \tau_D \frac{2^5\pi^3 n_r \mu_D^2 c}{3\hbar}\tilde{\nu}^3 L_D(2\pi c\tilde{\nu}), \tag{14}$$

$$I_A(2\pi c\tilde{\nu}) = \frac{3000(\ln 10) n_r \hbar}{(2\pi)^2 N_A \mu_A^2 \tilde{\nu}}\epsilon_A(\tilde{\nu}), \tag{15}$$

where τ_D is the lifetime of the spontaneous decay of $|D\rangle$ state, n_r is the refractive index of the medium, μ_D is the transition dipole for $|D\rangle \rightarrow |g\rangle$ transition, μ_A is the transition dipole for $|g\rangle \rightarrow |A\rangle$ transition, N_A is the Avogadro's number. Inserting the above expressions into Eq. (13), we find the following general expression for the rate of RET:

$$k_F = \frac{9000(\ln 10)}{128\pi^5 N_A \tau_D}\frac{J^2}{\mu_D^2\mu_A^2}\int_{-\infty}^{\infty} \mathrm{d}\,\tilde{\nu}\frac{f_D(\tilde{\nu})\epsilon_A(\tilde{\nu})}{\tilde{\nu}^4}. \tag{16}$$

If the distance between D and A is much larger than the length scales characteristic of their transition dipoles, the following dipole approximation can be made:

$$J = \frac{\boldsymbol{\mu}_D\cdot\boldsymbol{\mu}_A - 3(\boldsymbol{\mu}_D\cdot\hat{\mathbf{R}})(\boldsymbol{\mu}_A\cdot\hat{\mathbf{R}})}{n_r^2 R^3}, \tag{17}$$

where R is the distance between the donor and the acceptor and $\hat{\mathbf{R}}$ is the corresponding unit vector. Then

$$\frac{J^2}{\mu_D^2\mu_A^2} = \frac{\kappa^2}{n_r^4 R^6}, \tag{18}$$

where

$$\kappa = \frac{\boldsymbol{\mu}_D\cdot\boldsymbol{\mu}_A - 3(\boldsymbol{\mu}_D\cdot\hat{\mathbf{R}})(\boldsymbol{\mu}_A\cdot\hat{\mathbf{R}})}{\mu_D\mu_A}. \tag{19}$$

Inserting this into Eq. (16), we find the following celebrated expression derived by Förster[20]:

$$k_F = \frac{9000(\ln 10)\kappa^2}{128\pi^5 N_A \tau_D n_r^4 R^6}\left(\int \mathrm{d}\,\tilde{\nu}\frac{f_D(\tilde{\nu})\epsilon_A(\tilde{\nu})}{\tilde{\nu}^4}\right). \tag{20}$$

RECENT THEORETICAL DEVELOPMENTS

The success of Förster's rate expression, Eq. (20), lies in its apparent generality needing only experimentally measurable parameters and spectral functions. However, this also makes it easy to overlook the assumptions implicit in the theory. As was stated in the preceding section, it is based on four major assumptions, let alone the perturbation theory. These are as follows: (i) It assumes that the donor and acceptor are coupled to independent bath modes. (ii) The excited donor molecule is assumed to have been equilibrated with its environments before the energy transfer occurs. (iii) It is based on the so-called Condon approximation that the electronic coupling constant J is assumed to be independent of any nuclear motion. (iv) The donor and the acceptor consist of single chromophores. Among these, the issue (i) has been discussed in detail in previous works. Correction of this assumption[89–91] is not difficult given that detailed information on the nature of exciton–bath coupling is known (which can be non-trivial). Theories addressing (ii)–(iv) and the quantum coherence will be discussed in detail below.

Nonequilibrium FRET

If the energy transfer dynamics is fast, it can occur before the equilibration in the excited state becomes complete. In this case, the assumption of Eq. (8) cannot be justified and more general rate expression, Eq. (7), needs to be used. Inserting the inverse Fourier transform of $I_A(\omega)$ defined by Eq. (11) directly into Eq. (7), we obtain the following expression[90]:

$$k(t) = \frac{J^2}{\pi\hbar^2}\int_{-\infty}^{\infty}\mathrm{d}\,\omega\; I_A(\omega)\mathrm{Re}\left[\int_0^t dt' \mathrm{e}^{-i\omega t' + iE_D t'/\hbar} \times \frac{1}{Z_{bD}} Tr_{bD}\left\{\mathrm{e}^{i(H_{bD}+B_D)t/\hbar}\mathrm{e}^{-iH_{bD}t'/\hbar} \times \mathrm{e}^{-i(H_{bD}+B_D)(t-t')/\hbar}\mathrm{e}^{-\beta H_{bD}}\right\}\right]. \tag{21}$$

In the above expression, the time-integration involving the dynamics of the donor molecule can be expressed as the time-dependent emission profile of D^* in the absence of the acceptor.

Assume that the system only consists of the donor and its own bath. The Hamiltonian for D^*

 © 2012 John Wiley & Sons, Ltd.

and the bath is $H_D = (E_D + B_D)|D\rangle\langle D| + H_{b_D}$. If the donor is excited at time zero by a delta pulse, the initial density operator at $t = 0$ is $\rho(0) = |D\rangle\langle D|\rho^g_{b_D}$. Then, employing the same time-dependent perturbation theory with respect to the matter–radiation interaction Hamiltonian, the following expression for the time-dependent emission profile can be obtained[90]:

$$L_D(t,\omega) \equiv 2\mathrm{Re}\left[\int_0^t \mathrm{d}\,t' \mathrm{e}^{-i\omega t' + iE_D t'/\hbar} \times \frac{1}{Z_{b_D}} Tr_{b_D}\left\{\mathrm{e}^{i(H_{b_D}+B_D)t/\hbar}\mathrm{e}^{-iH_{b_D}t'/\hbar} \times \mathrm{e}^{-i(H_{b_D}+B_D)(t-t')/\hbar}\mathrm{e}^{-\beta H_{b_D}}\right\}\right]. \quad (22)$$

Inserting Eq. (22) into Eq. (21), we find the following expression for the nonequilibrium rate[90]:

$$k(t) = \frac{J^2}{2\pi\hbar^2}\int_{-\infty}^{\infty}\mathrm{d}\,\omega I_A(\omega)L_D(t,\omega). \quad (23)$$

In the limit where $t \to \infty$, this expression approaches Eq. (12) given that $L_D(\infty,\omega)$ approaches the emission lineshape in the stationary limit.

Inelastic FRET

It is reasonable to use the Condon approximation that the electronic coupling J in Eq. (3) is independent of nuclear coordinates if it indeed remains constant or fluctuates in a way independent of the electronic excitation dynamics without any energy exchange. In the latter case, averaging over the time-dependent fluctuations leads to a constant J. However, for the cases where the donor–acceptor pair is connected by a bridge molecule or locked in soft environments with significant quantum modes, the exchange of energy between the electronic excitation and the nuclear quantum degrees of freedom should be taken into consideration. Extension of FRET for this situation has been made.[88]

Assume that the bath Hamiltonian H_b can be decomposed into three components as follows:

$$H_b = H_{b_D} + H_{b_A} + H_{b_J}, \quad (24)$$

where H_{b_J} is the bath Hamiltonian governing the dynamics of J. If H_{b_J} is independent of all the degrees of freedom constituting the donor and the acceptor baths, and thus commutes with H_{b_D}, H_{b_A}, B_D, and B_A, a time-dependent perturbation theory can be used following similar steps as those leading to Eq. (12). As a result, one can obtain the following rate expression[88]:

$$k_{IF} = \frac{1}{2\pi\hbar^2}\int_{-\infty}^{\infty}\mathrm{d}\,\omega\int_{-\infty}^{\infty}\mathrm{d}\,\omega' L_D(\omega)I_A(\omega')K_J(\omega-\omega'), \quad (25)$$

where

$$K_J(\omega) = \frac{1}{\pi}\mathrm{Re}\int_0^{\infty}\mathrm{d}\,t\ \mathrm{e}^{i\omega t} Tr_{b_J}\left\{\mathrm{e}^{iH_{b_J}t/\hbar}J\,\mathrm{e}^{-iH_{b_J}t/\hbar}J\rho_{b_J}\right\}. \quad (26)$$

The form of Eq. (25) is generic for inelastic processes where the exchange of energy between transferring excitation and the modulating degrees of freedom is possible. Introducing

$$\tilde{K}_J(\tilde{\nu}) = 2\pi c K_J(2\pi c\tilde{\nu}), \quad (27)$$

and inserting Eqs. (14) and (15) into Eq. (25), we find an expression analogous to Förster's expression as follows:

$$k_{IF} = \frac{9000(\ln 10)}{128\pi^5 N_A \tau_D \mu_D^2 \mu_A^2} \times \int \mathrm{d}\tilde{\nu}\int \mathrm{d}\tilde{\nu}'\frac{f_D(\tilde{\nu})\epsilon_A(\tilde{\nu}')}{\tilde{\nu}^3\tilde{\nu}'}\tilde{K}_J(\tilde{\nu}-\tilde{\nu}'). \quad (28)$$

Equation (20) corresponds to the limit of the above expression, where $\tilde{K}_J(\tilde{\nu})$ approaches the delta function and modulation of J is caused by orientational fluctuation, i.e., $\tilde{K}_J(\tilde{\nu}-\tilde{\nu}') \approx \mu_D^2\mu_A^2\kappa^2\delta(\tilde{\nu}-\tilde{\nu}')/(n_r^4 R^6)$. Equation (28) can be extended further to include the nonequilibrium effect and effects of common modes.[88]

Multichromophoric FRET

In natural light harvesting complexes or synthetic multichromohpore systems, it is common to find transfer of excitons delocalized over multiple chromophores or sites. As long as the group of donor molecules in these systems is well separated from that of acceptor molecules, a rate description based on the FGR formula can be justified.

Assume that the system consists of two distinctive sets of chromophores, donors (D_j, $j = 1,\ldots,N_D$) and acceptors (A_k, $k = 1,\ldots,N_A$). The state where all the D_js and A_ks are in their ground electronic states is denoted as $|g\rangle$. The state where D_j is excited while all other remain in the ground electronic state is denoted as $|D_j\rangle$. The state $|A_k\rangle$ is defined similarly. All the rest degrees of freedom such as molecular vibrations and solvation coordinates are termed as bath. The bath Hamiltonian is assumed to be $H_b = H_{b,D} + H_{b,A}$, where the subscripts D and A, respectively, denote the components coupled to the set of donors and acceptors.

The excitation dynamics is assumed to be much faster than the spontaneous decay of the excited state, which is neglected. Thus, the single exciton

 © 2012 John Wiley & Sons, Ltd.

Hamiltonians of D and A are

$$H_{e,D} = \sum_{j=1}^{N_D} E_{Dj}|D_j\rangle\langle D_j| + \sum_{j\neq j'} \Delta^D_{jj'}|D_j\rangle\langle D_{j'}|, \quad (29)$$

$$H_{e,A} = \sum_{k=1}^{N_A} E_{Ak}|A_k\rangle\langle A_k| + \sum_{k\neq k'} \Delta^A_{kk'}|A_k\rangle\langle A_{k'}|, \quad (30)$$

where $\Delta^D_{jj'}$ and $\Delta^A_{kk'}$ are assumed to be real numbers. The resonance interaction between $|D_j\rangle$ and $|A_k\rangle$ is represented by

$$H_{DA} = \sum_{j=1}^{N_D}\sum_{k=1}^{N_A} J_{jk}(|D_j\rangle\langle A_k| + |A_k\rangle\langle D_j|), \quad (31)$$

where J_{jk} is assumed to be independent of any bath coordinates. The excitation-bath coupling is assumed to be diagonal in the site excitation basis as follows:

$$\begin{aligned} H_{eb} &= \sum_{j=1}^{N_D} B_{Dj}|D_j\rangle\langle D_j| + \sum_{k=1}^{N_A} B_{Ak}|A_k\rangle\langle A_k| \\ &\equiv H_{eb,D} + H_{eb,A}, \end{aligned} \quad (32)$$

where B_{Dj} and B_{Ak} are bath operators coupled to $|D_j\rangle$ and $|A_k\rangle$, respectively. These operators and the bath Hamiltonian can be arbitrary except that all the bath modes coupled to $|D_j\rangle$s are independent of those coupled to $|A\rangle_k$s. Thus, the total Hamiltonian can be expressed as

$$H = H_D + H_A + H_{DA}, \quad (33)$$

where

$$H_D \equiv H_{e,D} + H_{b,D} + H_{eb,D}, \quad (34)$$

$$H_A \equiv H_{e,A} + H_{b,A} + H_{eb,A}. \quad (35)$$

Assume the situation where a donor exciton is populated by an impulsive pulse at $t = 0$, before which all the chromophores have been in the ground electronic states and the bath in thermal equilibrium. As in the single chromophoric case, the duration of pulse is assumed to be short and can be approximated well by a delta function. Then, the density operator of the system plus the bath after the excitation by the pulse can be approximated as

$$\rho(0) = |D_{\hat{\mathbf{e}}}\rangle\langle D_{\hat{\mathbf{e}}}|\rho^g_{b_D}\rho^g_{b_A}, \quad (36)$$

where $|D_{\hat{\mathbf{e}}}\rangle = \hat{\mathbf{e}}\cdot\sum_j \boldsymbol{\mu}_{D_j}|D_j\rangle$, with $\hat{\mathbf{e}}$ being the polarization of the impulsive pulse and $\boldsymbol{\mu}_{D_j}$ the transition dipole moment vector of D_j, $\rho^g_{bD} = \mathrm{e}^{-\beta H_{b,D}}/Tr_{b_D}\{\mathrm{e}^{-\beta H_{b,D}}\}$, and $\rho^g_{bA} = \mathrm{e}^{-\beta H_{b,A}}/Tr_{b_A}\{\mathrm{e}^{-\beta H_{b,A}}\}$.

Employing the same time-dependent perturbation as deriving Eq. (21), we obtain the following rate expression[43]:

$$k(t) = \sum_{j'j''}\sum_{k'k''} \frac{J_{j'k'}J_{j''k''}}{2\pi\hbar^2}\int_{-\infty}^{\infty} \mathrm{d}\,\omega I_A^{k'k''}(\omega)L_D^{j''j'}(t,\omega), \quad (37)$$

where $I_A^{k'k''}(\omega)$ and $L_D^{j''j'}(t;\omega)$ represent absorption of acceptors and the stimulated emission of donors and are defined as

$$\begin{aligned} I_A^{k'k''}(\omega) \equiv \int_{-\infty}^{\infty} \mathrm{d}\,t\,\mathrm{e}^{i\omega t} \\ \times Tr_{bA}\left\{\langle A_{k'}|\mathrm{e}^{iH_{b,A}t'/\hbar}\,\mathrm{e}^{-iH_At'/\hbar}\rho^g_{b_A}|A_{k''}\rangle\right\}, \end{aligned} \quad (38)$$

$$\begin{aligned} L_D^{j''j'}(t;\omega) \equiv 2\mathrm{Re}\Bigg[\int_0^t \mathrm{d}\,t'\,\mathrm{e}^{-i\omega t'} \\ \times\, Tr_{bD}\Big\{\langle D_{j''}|\mathrm{e}^{-iH_{b,D}t'/\hbar}\,\mathrm{e}^{-iH_D(t-t')/\hbar} \\ \times\, |D_{\hat{\mathbf{e}}}\rangle\langle D_{\hat{\mathbf{e}}}|\rho^g_{b_D}\,\mathrm{e}^{iH_Dt/\hbar}|D_{j'}\rangle\Big\}\Bigg]. \end{aligned} \quad (39)$$

In the stationary limit of $t\to\infty$, $k(t)$ approaches the following multichromophoric-FRET (MC-FRET) rate expression:

$$k_{MF} = \sum_{j'j''}\sum_{k'k''} \frac{J_{j'k'}J_{j''k''}}{2\pi\hbar^2}\int_{-\infty}^{\infty} \mathrm{d}\,\omega I_A^{k'k''}(\omega)L_D^{j''j'}(\infty,\omega). \quad (40)$$

Under the assumption that the dynamics in the excitonic manifold is ergodic, we find that

$$\begin{aligned} L_D^{j''j'}(\infty,\omega) = 2\mathrm{Re}\int_0^{\infty} \mathrm{d}\,t\;\mathrm{e}^{-i\omega t} \\ \times Tr_{bD}\left\{\langle D_{j''}|\mathrm{e}^{-iH_{b,D}t/\hbar}\rho^e_{D,b}\,\mathrm{e}^{iH_Dt/\hbar}|D_{j'}\rangle\right\}, \end{aligned} \quad (41)$$

where $\rho^e_{D,b} = \mathrm{e}^{-\beta H_D}/Tr\{\mathrm{e}^{-\beta H_D}\}$ is the canonical density operator of donors and the bath in the single exciton manifold. Sumi's starting expression in his MC-FRET theory[92] is equivalent to Eq. (40) with the above expression of emission lineshape.

Coherent Resonance Energy Transfer

Quantum coherence is an issue that has been drawing significant experimental[13,16,39,53,93–95] and theoretical[96–104] attention lately. Two-dimensional electronic spectroscopy on natural photosynthetic systems[53–55] and conjugated polymers[16] reported time domain measurement of long lasting quantum coherence despite substantial disorder and relaxation processes. In soft macromolecules such as natural photosynthetic and conjugated polymer systems, multitudes of electronic and nuclear dynamical processes render it difficult to make clear separation of timescales. For quantitative analysis and assessment of quantum

 © 2012 John Wiley & Sons, Ltd.

coherence in RET processes occurring in such systems, theory needs to go beyond the assumption of incoherent quantum transfer[21,43,88,90105] and the approximation of weak system-bath coupling[106–108] because the strengths of electronic and electron–phonon coupling are comparable in this so-called intermediate coupling regime. New theoretical approaches addressing these issues have been developed by a number of groups.[96,97,99–102] Among these, we present a brief overview of polaronic quantum master equation (PQME) approach[96,109–113] developed for general multistate-boson Hamiltonian.[110,113]

The concept of small polaron was pioneered by Holstein[114] to treat charge transfer in organic molecular crystals in the 1960s and later extended by Silbey and coworkers[115–121] to treat RET in the 1970s. This provides a general framework that yields accurate results in both strong and weak electron–phonon coupling limits, although the coherent version of the dynamical equations has never been developed in the literature. Instead of treating the electronic and vibrational degrees of freedom separately, the polaronic approach adopts a fundamentally different picture for RET. Through the application of a polaron transformation, a combined electronic/vibrational basis called polaron states is used to describe the RET dynamics, thus considering the electronic excitation that moves collectively with its surrounding bath deformation as the zeroth-order state.

Consider a group of N chromophores embedded in protein or solid medium not necessarily crystalline. Let us assume that the single exciton space of chromophores defines the system. Then, the system Hamiltonian can be expressed as

$$H_s = \sum_{l=1}^{N} E_l |l\rangle\langle l| + \sum_{l\neq l'}^{N} J_{ll'} |l\rangle\langle l'|, \tag{42}$$

where $|l\rangle$ represents the state where only the lth chromophore is excited and E_l is its excitation energy. $J_{ll'}$ is the electronic coupling between states $|l\rangle$ and $|l'\rangle$. The rest degrees of freedom are defined as the bath, which are approximated as linearly coupled harmonic oscillators. Thus, $H_b = \sum_n \hbar\omega_n (b_n^\dagger b_n + \frac{1}{2})$ and $H_{sb} = \sum_{l=1}^{N} \sum_n \hbar\omega_n g_{n,l} (b_n + b_n^\dagger) |l\rangle\langle l|$. Then, the total Hamiltonian governing the dynamics of system and bath can be written as follows:

$$H = H_s + H_{sb} + H_b. \tag{43}$$

The total density operator of system and bath, which is denoted as $\rho(t)$, is governed by the following quantum Liouville equation:

$$\frac{\mathrm{d}}{\mathrm{d}t}\rho(t) = -i\mathcal{L}\rho(t) = -\frac{i}{\hbar}[H, \rho(t)]. \tag{44}$$

The exact solution of this is not possible in general and approximation needs to be made.

Polaron transformation[114–120] can be used to construct a quantum master equation (QME) that is applicable beyond weak system-bath coupling utilizing the fact that the resulting system-bath couplings after the transformation are of bounded exponential form. Consider the following polaron transformation of the total Hamiltonian:

$$\tilde{H} = \mathrm{e}^{G} H e^{-G} = \tilde{H}_s + \tilde{H}_{sb} + H_b, \tag{45}$$

where $G = \sum_{l=1}^{N} \sum_n g_{n,l} (b_n^\dagger - b_n) |l\rangle\langle l|$. Here, we can define a new zeroth-order Hamiltonian

$$\tilde{H}_0 = \tilde{H}_s + \langle \tilde{H}_{sb} \rangle_b + H_b = \tilde{H}_{0,s} + H_b, \tag{46}$$

where $\langle \ldots \rangle_b$ means average over the bath in equilibrium and $\tilde{H}_{0,s} = \tilde{H}_s + \langle \tilde{H}_{sb} \rangle_b$. Then, define the following interaction picture and polaron transformed total density operator.

$$\tilde{\rho}_I(t) = \mathrm{e}^{i\tilde{H}_0 t/\hbar} e^{G} \rho(t)\, \mathrm{e}^{-G}\, \mathrm{e}^{-i\tilde{H}_0 t/\hbar}. \tag{47}$$

The corresponding reduced system density operator is defined as

$$\tilde{\sigma}_I(t) \equiv Tr_b \{\tilde{\rho}_I(t)\}. \tag{48}$$

Then, employing the standard projection operator technique, the following form of time evolution equation can be derived:

$$\frac{\mathrm{d}}{\mathrm{d}t}\tilde{\sigma}_I(t) = -\mathcal{R}(t)\tilde{\sigma}_I(t) + \mathcal{I}(t), \tag{49}$$

where $\mathcal{R}(t)$ accounts for the relaxation and dephasing of the system and $\mathcal{I}(t)$ the contribution of nonequilibrium initial distribution. Explicit expressions for $\mathcal{R}(t)$ and $\mathcal{I}(t)$ valid up to the second order of $\tilde{H}_{sb} - \langle \tilde{H}_{sb} \rangle_b$ has been derived.[109]

Once the reduced system density operator in the interaction picture, $\tilde{\sigma}_I(t)$, is determined, the population at the lth site can be calculated by

$$p_l(t) = \mathrm{Tr}_s \left\{ P_{l,I}(t) \tilde{\sigma}_I(t) \right\}, \tag{50}$$

where $P_{l,I}(t) = \mathrm{e}^{i\tilde{H}_{0,s}t/\hbar} |l\rangle\langle l| \mathrm{e}^{-i\tilde{H}_{0,s}t/\hbar}$.

The PQME approach for coherent resonance energy transfer (CRET) explained above is an elegant way to describe non-Markovian dynamics, coherence (off-diagonal density matrix element) dynamics, and multiphonon effects. In addition, it can be extended for more general forms of system–bath interactions. Thus, it goes beyond perturbation theory while being tractable, and will be able to play a critical role for our

 © 2012 John Wiley & Sons, Ltd.

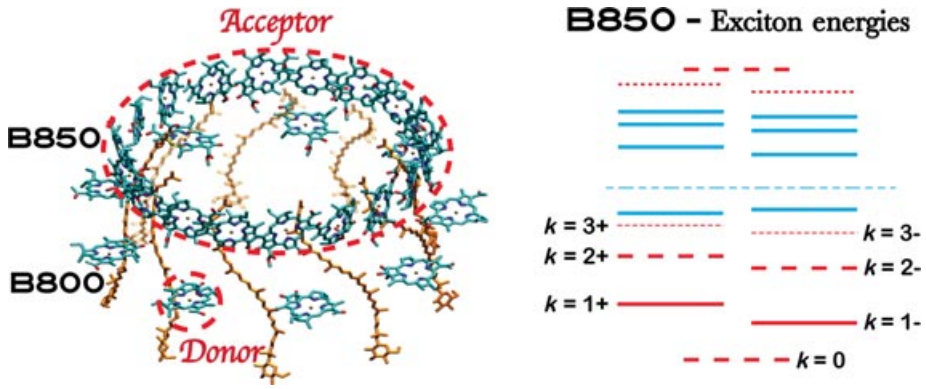

FIGURE 1 | The arrangement of chromophores in the LH2 of *Rps. Acidophila* (left figure) and the energy level diagram of a typical B850 exciton band (right figure). In this diagram, solid red lines represent major bright states and dashed red lines represent weakly bright states.

understanding of how coherence between excitonic states affect the excitation energy transfer and how protein dynamics is coupled to the RET dynamics between chromophores in photosynthetic complexes.

APPLICATIONS

Photosynthetic Light Harvesting Complex 2

This section reviews recent applications[43,44,122] of the MC-FRET theory to the energy transfer within the LH2 of *Rhodopseudomonas (Rps.) acidophila*. Figure 1 shows the structure and the arrangement of chromophores in LH2, which was determined by Cogdell and coworkers.[8,123] The structure reveals remarkable symmetry in the arrangement of bacteriochlorophylls (BChls), in which 27 BChls (type *a*) are arranged into two highly symmetric rings: 18 of them form the so-called B850 ring that is responsible for the absorption band with a maximum at 850 nm, and the other 9 form the B800 ring that absorbs maximally at about 800 nm. The center-to-center distance between adjacent B850 BChls is about 9.6 Å, which results in moderately strong nearest-neighbor couplings of about -300 cm^{-1}. The center-to-center distance between BChls in the B800 ring is about 21 Å, leading to relatively weak nearest-neighbor electronic couplings of about -25 cm^{-1}.

The total Hamiltonian of the system can be expressed as

$$H = E_g|g\rangle\langle g| + H_A + H_D + H_{DA}, \qquad (51)$$

where $|g\rangle$ is the ground electronic state where none of the BChls in B850 and B800 is excited and E_g is the corresponding energy. H_A is the acceptor (B850) Hamiltonian and represents the entire B850 unit, H_D is the donor (B800) Hamiltonian, and H_{DA} represents the electronic coupling between the donor and the acceptor. Let us define H_A^0 as the Hamiltonian representing only single exciton states of B850. Thus,

$$H_A^0 = \sum_{n=1}^{18} E_n|n\rangle\langle n| + \sum_{n\neq m} \Delta(n-m)|n\rangle\langle m|, \qquad (52)$$

where $|n\rangle$ is the state where nth BChl of B850 is excited (Q_y transition) whereas all other BChls are in the ground state and E_n is the corresponding energy. We here use the convention that odd n represents an α-BChl and even n a β-BChl. $\Delta(n-m)$ is the electronic coupling between states $|n\rangle$ and $|m\rangle$, for which a complete set of values[124] is available.

Within the approximation of bosonic bath, the total acceptor Hamiltonian can be expressed as

$$H_A = H_A^0 + \sum_{n=1}^{18}\sum_{k\in B_A} \hbar\omega_k g_{k,n}(b_k^\dagger + b_k)|n\rangle\langle n| + \sum_{k\in B_A} \hbar\omega_k (b_k^\dagger b_k + \frac{1}{2}), \qquad (53)$$

where ω_k is the frequency of the kth bath harmonic oscillator in the set of the acceptor bath B_A, $g_{k,n}$ represents the strength of its coupling to $|n\rangle$, and $b_k^\dagger$ and b_k are corresponding raising and lowering operators.

The eigenstates and the lineshape expression for the B850 unit have been studied in detail.[124] Since the symmetry element of the B850 unit contains two BChls (one α and one β), the eigenstates of H_A^0 consist of two bands,[125] denoted upper and lower. Each band has nine electronic states. In the absence of disorder, the states in each band can be labeled according to their cyclic symmetry, ranging from 0 to 8. In actual system, this symmetry is broken because each BChl has different excitation energy and local environment.[125] A typical energy diagram including the effect of disorder is shown in Figure 1. We denote

 © 2012 John Wiley & Sons, Ltd.

the eigenstates of H_A^0 as $|\psi_{l,p}\rangle$ and $|\psi_{u,p}\rangle$, where $p = 0, \ldots, 8$ and l (u) represents the lower (upper) band. Then, H_A^0 can be expressed as

$$H_A^0 = \sum_{p=0}^{8} \left\{ \mathcal{E}_{l,p} |\psi_{l,p}\rangle\langle\psi_{l,p}| + \mathcal{E}_{u,p} |\psi_{u,p}\rangle\langle\psi_{u,p}| \right\}, \quad (54)$$

where, for $p < p'$, $\mathcal{E}_{l,p} < \mathcal{E}_{l,p'}$ and $\mathcal{E}_{u,p} > \mathcal{E}_{u,p'}$. Let us introduce a transformation matrix $\mathcal{C}$ relating the local excitation states to the above eigenstates as follows:

$$|n\rangle = \sum_{p=0}^{8} \left\{ \mathcal{C}_{l,p}^n |\psi_{l,p}\rangle + \mathcal{C}_{u,p}^n |\psi_{u,p}\rangle \right\}, \quad (55)$$

where $\mathcal{C}_{l,p}^n = \langle n|\psi_{l,p}\rangle$ and $\mathcal{C}_{u,p}^n = \langle n|\psi_{u,p}\rangle$. Given the parameters of H_A^0 for a specific B850 unit, the eigenvalues and eigenvectors in Eq. (54), and the transformation matrix in Eq. (55) can be determined simultaneously through numerical matrix diagonalization of H_A^0.

Assuming that each BChl in B850 has the same spectral density, the following form can be used to characterize the exciton–phonon coupling:

$$\mathcal{J}(\omega) = \sum_{k \in B_A} \delta(\omega - \omega_k) \omega_k^2 g_{k,n}^2 = 0.22 \omega e^{-\omega/\omega_{c1}} + 0.78 \frac{\omega^2}{\omega_{c2}} \mathrm{e}^{-\omega/\omega_{c2}} + 0.31 \frac{\omega^3}{\omega_{c3}^2} \mathrm{e}^{-\omega/\omega_{c3}}, \quad (56)$$

where $\omega_{c1} = 170\,\mathrm{cm}^{-1}$, $\omega_{c2} = 34\,\mathrm{cm}^{-1}$, and $\omega_{c3} = 69\,\mathrm{cm}^{-1}$. This spectral density is based on that determined by Renger and Marcus[126] from fluorescence line narrowing experiment of the related B777-complex.

Let us first approximate the donor as the single chromophore in the B800 unit as drawn in Figure 1. This simplification is based on the fact that the electronic couplings between BChls in B800 are much smaller than those in B850. But as will be shown below, coherence in B800 can have subtle but important effect. With this point in mind, for now, we can assume the donor and its bath Hamiltonian consists of three terms as follows:

$$H_D = E_D |D\rangle\langle D| + \sum_{k \in B_D} \hbar\omega_k g_k (b_k^\dagger + b_k) |D\rangle\langle D| + \sum_{k \in B_D} \hbar\omega_k \left(b_k^\dagger b_k + \frac{1}{2} \right), \quad (57)$$

where $|D\rangle$ corresponds to the state where the BChl representing the B800 is excited and E_D is its energy, ω_k is the frequency of the kth oscillator in the set of the donor bath B_D, g_k is the magnitude of its coupling to $|D\rangle$, and $b_k^\dagger$ and b_k are the raising and lowering operators of the kth oscillator. It was found that the following approximation for the spectral density for B800 can reproduce the lineshape of B800 within this single BChl representation[44]:

$$\mathcal{J}_D(\omega) \equiv \sum_{k \in B_D} \delta(\omega - \omega_k) \omega_k^2 g_k^2 = 0.7 \mathcal{J}(\omega). \quad (58)$$

The electronic coupling Hamiltonian H_{DA} in Eq. (51) is given by

$$H_{DA} = \sum_{n=1}^{18} J_n (|D\rangle\langle n| + |n\rangle\langle D|), \quad (59)$$

where J_n can be approximated as the transition dipole interaction between $|D\rangle$ and $|n\rangle$ as follows:

$$J_n = \frac{\boldsymbol{\mu}_D \cdot \boldsymbol{\mu}_n - 3(\boldsymbol{\mu}_D \cdot \hat{\mathbf{R}}_n)(\boldsymbol{\mu}_n \cdot \hat{\mathbf{R}}_n)}{n_r^2 R_n^3}. \quad (60)$$

In this expression, R_n is the distance between the donor and the nth acceptor, $\hat{\mathbf{R}}_n$ is the corresponding unit distance vector, $\boldsymbol{\mu}_D$ is the transition dipole for $|g\rangle \rightarrow |D\rangle$ (the excitation of the BChl in B800), and $\boldsymbol{\mu}_n$ is that for $|g\rangle \rightarrow |n\rangle$ (the excitation of nth BChl in B850). All the transition dipole vectors are assumed to have the same magnitude, $\mu = |\boldsymbol{\mu}_D| = |\boldsymbol{\mu}_n|$.

The MC-FRET rate expression, Eq. (40), when applied to the present system, can be expressed as

$$k_{B800 \rightarrow B850} = \sum_{n,n'=1}^{18} \frac{J_n J_{n'}}{2\pi\hbar^2} \int_{-\infty}^{\infty} \mathrm{d}\,\omega I_{A,nn'}(\omega) L_D(\omega), \quad (61)$$

where

$$L_D(\omega) = \int_{-\infty}^{\infty} \mathrm{d}\,t\ \mathrm{e}^{i(\omega - \epsilon_D + \epsilon_g)t} \mathrm{e}^{-0.7 \int_0^\infty \mathrm{d}\,\omega \frac{\mathcal{J}(\omega)}{\omega^2} \left\{ \coth\left(\frac{\hbar\omega}{2k_B T}\right)(1 - \cos(\omega t)) - i \sin(\omega t) \right\}}, \quad (62)$$

$$I_{A,nn'}(\omega) \equiv \int_{-\infty}^{\infty} \mathrm{d}\,\tau\ \mathrm{e}^{i\omega\tau}\, Tr_{bA} \left\{ \langle n| \mathrm{e}^{i H_{b,A}\tau/\hbar}\, \mathrm{e}^{-i H_A \tau/\hbar} \rho_{b_A}^g |n'\rangle \right\}. \quad (63)$$

In the above expression, Tr_{bA} is the trace over the basis of the acceptor bath Hamiltonian $H_{b,A}$ and $\rho_{b_A}^g = \mathrm{e}^{-\beta H_{b,A}} / Tr_{bA}\{\mathrm{e}^{-\beta H_{b,A}}\}$.

Let us introduce the following linear combination of the acceptor states weighted by J_n:

$$|J\rangle = \sum_{n=1}^{18} J_n |n\rangle. \quad (64)$$

 © 2012 John Wiley & Sons, Ltd.

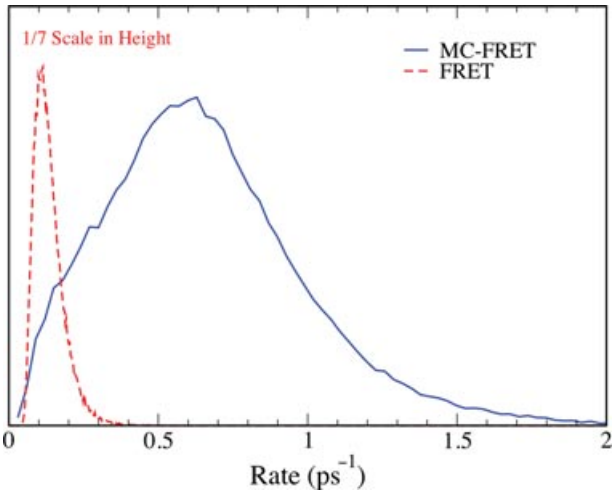

FIGURE 2 | Distribution of rates based on the MC-FRET and FRET (see also Ref 44)

Invoking the approximation of the second-order time nonlocal QME,[124] Equation (61) can be expressed as

$$\sum_{n,n'=1}^{18} J_n J_{n'} I_{A,nn'}(\omega) \approx -\frac{1}{\pi}\mathrm{Im}Tr_A\left\{\frac{|J\rangle\langle J|}{\omega+(E_g-H_A^0)/\hbar+i\hat{\mathcal{K}}(\omega)}\right\}\equiv J_A(\omega), \tag{65}$$

where

$$\hat{\mathcal{K}}(\omega)=\sum_{n=1}^{18}\sum_{p=0}^{8}\sum_{b=l}^{u}\hat{\kappa}(\omega-\mathcal{E}_{b,p}/\hbar)|C_{b,p}^n|^2|n\rangle\langle n|, \tag{66}$$

with

$$\hat{\kappa}(\omega)\equiv\int_0^\infty \mathrm{d}\,t\;\mathrm{e}^{i\omega t}\int_0^\infty \mathrm{d}\,\omega\mathcal{J}(\omega)\times\left\{\coth\left(\frac{\hbar\omega}{2k_BT}\right)\cos(\omega t)-i\sin(\omega t)\right\}. \tag{67}$$

Then, the MC-FRET rate expression equation (61) can be simplified to

$$k_{B800\to B850}\approx\frac{1}{2\pi\hbar^2}\int_{-\infty}^{\infty}J_A(\omega)L_D(\omega). \tag{68}$$

Evaluation of this rate expression can be made by calculating $J_A(\omega)$ and $L_D(\omega)$ at discrete values of ω and performing numerical integration.

At the simplest level, the disorder in LH2 can be modeled by Gaussian disorder in three energies, E_n, E_g, and E_D. For the B850 unit, the standard deviations for E_n and E_g are 250 and 40 cm^{-1}. For the B800 unit, the standard deviation for $E_D - E_g$ is 54 cm^{-1} and the average bias of the excitation energy of the B800-BChl relative to that of B850-BChl, $\langle E_D - E_n\rangle$ is 260 cm^{-1}. These choices are based on the fitting of low-temperature ensemble lineshape. In all the calculations of the ensemble lineshape and the energy transfer rate shown below, a low-temperature limit of $k_BT = 10\,\mathrm{cm}^{-1}$ is assumed. Figure 2 shows the resulting distribution of rates in units of ps^{-1}. Comparison is also made with the hypothetical distribution of FRET rates treating the B850 as a single chromophore. In both calculations, it was assumed that each BChl has the same value of $\mu/n_r = 5.3$ Debye (D). This choice was made by assuming that the average rate calculated from the distribution of MC-FRET rates is equal to the experimental rate at 4 K,[127] which is $(1.5\,\mathrm{ps})^{-1}$. Assuming that the optical dielectric response of the protein medium is $\epsilon = 1.5 - 2$, we find that $\mu = 6.5 - 7.5$ D, which is comparable to experimental results.[127–129]

As can be seen clearly from Figure 2, the rates based on Eq. (68) are much larger and more dispersive than those based on FRET. The most probable rate of the former is about five times larger than the latter, which is consistent with known discrepancies between experimental and FRET rates. The major source of the enhancement is the contribution of dark coherent exciton states of B850, which are in tune with the energy of the B800 unit. Although this fact had been recognized in previous applications based on the sum-over-exction states approach,[130,131] the above result[44] provides more definitive and clear theoretical understanding.

The energy difference between the B800 and B850 units comes from the excitonic delocalization of the B850 band, on the one hand, and the fact that the BChl in the former has higher excitation energy than the latter (about 260 cm^{-1}). It is interesting to see whether this difference has any biological implication. Calculation has been made for the distributions of both MC-FRET rates and the original FRET rates for six other values of the energy difference. For each choice of bias, the values of $\tau = 1/k_{av}$, where k_{av} is the average of the distribution of k_{MF}s or k_Fs, are plotted in Figure 3. It is important to note that the transfer time based on MC-FRET is quite insensitive to the bias up to about 400 cm^{-1}, whereas that based on FRET varies over an order of magnitude. Thus, the MC effects make the transfer time insensitive to changes in energy bias. This indicates that the purple bacteria are utilizing the MC effect to almost the greatest extent to guarantee the irreversibility of the energy flow from B800 to B850 while not affecting the transfer time significantly. Thus, the MC-FRET theory provides clear rationale for relative band positions of the B800 and B850 exciton states.

 © 2012 John Wiley & Sons, Ltd.

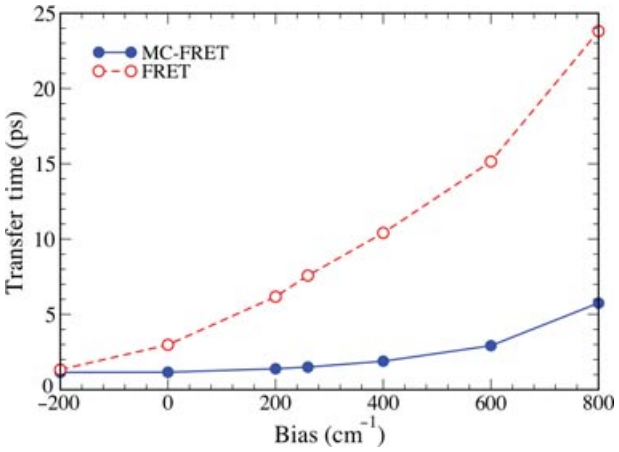

FIGURE 3 | Plot of average transfer times versus the bias (see also Ref 44).

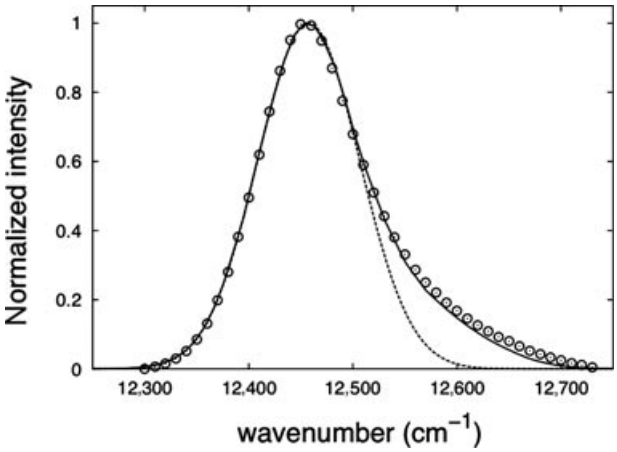

FIGURE 4 | Spectral lineshape calculated for an ensemble of the B800 rings from *Rps. acidophila* including static disorder and quantum coherence effect.[122] We compare the simulated spectrum (solid line) with the experimental absorption spectrum at 6 K (open circle). A Gaussian fit to the red side of the simulated spectrum (dashed line) is also presented to show that the long tail at the blue side of the band cannot be explained by a Gaussian inhomogeneous lineshape.

The results[43,44] reviewed above demonstrate the MC effects within the B850 unit. However, the MC effect within B800 can be significant as well although in a subtle way.[122] Typically, B800 excitations are considered as localized on individual pigments as depicted in Figure 1 because the electronic couplings between B800 BChls are smaller than the energetic disorder in the system. However, a detailed investigation of the low-temperature spectrum of the B800 band revealed that coherence in the B800 ring subtly changes both the spectrum and RET dynamics in the LH2 complex.[122] Figure 4 shows the experimental low-temperature B800-only ensemble spectrum together with a simulation of the spectral lineshape for an ensemble of B800 rings. The simulation was based on a model of 9 B800-BChls with modest nearest neighbor excitonic coupling:

$$H_{B800} = \sum_{n=1}^{9} E_n |n\rangle\langle n| + \sum_{n-m=\pm 1} J_{nm} |n\rangle\langle m|. \quad (69)$$

To model static disorder, E_n and J are treated as having random components:

$$E_n = E(0) + \delta E_I + \delta E_D(n), \quad (70)$$

$$J_{n,n+1} = J(0) + \delta J(n). \quad (71)$$

where $E(0)$ and $J(0)$ are ensemble-averaged site energy and nearest neighbor electronic coupling, respectively. δE_I, $\delta E_D(n)$, and $\delta J(n)$ are independent Gaussian random variables with zero mean and standard deviations σ_I, σ_D, and σ_J, respectively. By fitting to the experimental spectrum, these disorder parameters were determined as follows: $\sigma_I = 10 \pm 5$ cm^{-1}, $\sigma_D = 60 \pm 10$ cm^{-1}, and $\sigma_J = 15 \pm 5$ cm^{-1}. The fit indicates that the off-diagonal disorder $\delta J(n)$ cannot be ignored. Moreover, the excellent agreement with the experimental data shown in Figure 4 indicates that the effect of coherence exists in the B800 ring and results in the asymmetric lineshape with a pronounced tail in the blue side of the band. The modeling suggests that because the B800 excitations are coherently delocalized on multiple BChls, the redistribution of dipole moments in the B800 exciton manifold leads to the asymmetric lineshape. Based on the calculated participation ratio in the simulations, it was determined that a majority of the B800 states are delocalized on 2–4 pigments. The calculation clearly shows that despite strong energetic disorder, the coherence in the B800 ring cannot be neglected, and the pronounced blue tail of the B800 band at low temperatures can be attributed as a signature of quantum coherence. Interestingly, the room temperature B800 absorption spectrum also exhibits a blue tail, suggesting that the higher temperatures do not fully destroy the coherence in the B800 ring. Note that the electron–phonon coupling and other dynamical effects were neglected in this modeling of lineshape. In principle, couplings to intra- and intermolecular vibrational modes of the B800 BChl molecules could also lead to a blue tail in the absorption band. While the contribution of vibrational couplings to the asymmetric shape of the B800 band remains to be examined in more details, several previous studies have indicated that the B800 spectrum cannot be explained solely by a simple theory including experimentally measured homogeneous lineshape function.[132,133] Clearly, a significant

 © 2012 John Wiley & Sons, Ltd.

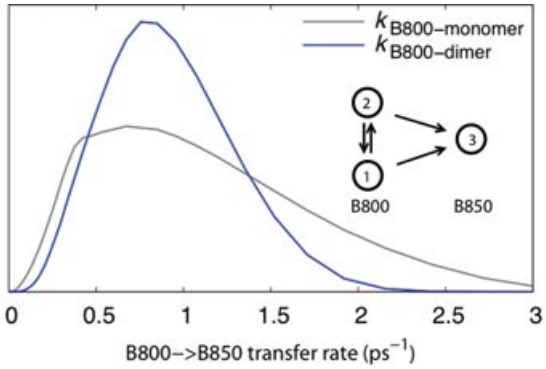

FIGURE 5 | A comparison of the distributions of the average B800 → B850 RET rate predicted by a B800 dimer model and a B800 monomer model. The theoretical B800 → B850 RET rate at $k_BT = 10\,cm^{-1}$ is calculated from the MC-FRET theory. The insert is a schematic of RET pathways in the B800 dimer model, showing alternative pathways when the coherence enables rapid energy transfer between the two B800 states.

portion of the asymmetric lineshape is due to the electronic coherence in the B800 excitations.

The MC effect caused by the quantum coherence in B800 ring also influences the B800 → B850 RET dynamics. Since a great portion of the B800 states are delocalized on two pigments across a wide regime of the B800 band, a coherent exciton delocalized on a pair of nearest-neighbor BChls presents a more realistic model for the B800 excited state at low temperatures. To study the MC effect of B800 on the B800 → B850 RET dynamics, theoretical rates for two simplified models for B800, a monomer BChl monomer and a dimer of BChls, were calculated.[122] In these calculations, the second-order time-nonlocal QME lineshape expression in Eq. (65)–(79) was used, and the spectral function in Eq. (58) was employed for the B800 BChl molecule. For the B850 BChls, the spectral density in Eq. (68) and the effective Hamiltonian for LH2 in Refs 134 and 135 were adopted. A simulation of the B850 linear absorption spectrum at 6 K was carried out to confirm that the model indeed reproduces well the B850 spectrum when the standard deviations for Gaussian disorder in E_n and E_g are set to 200 and $50\,cm^{-1}$, respectively. Figure 5 shows the distributions of B800 → B850 RET rates calculated based on the model and the MC-FRET theory (Eq. (40)). The dimer calculations indicate that coherence allows rapid intraband transfer between B800 BChls to provide alternative RET pathways when a direct transfer to the B850 is slow. As a result, the B800 coherence makes the B800 → B850 RET rate more uniform and hence more robust against energetic disorder in the system. Along with the results shown in Figures 2 and 3, it was suggested that the MC effects due to coherent delocalization of the donor and acceptor exctions can be responsible for the optimization of the natural system that helps the RET dynamics efficient and robust against energetic disorder.[122]

To summarize, the energy tuning and spectral characteristics of the B850 system depend critically on the quantum coherence induced by the strong intraring excitonic couplings in the system. The efficient B800 intraband RET, due to the B800 coherence, is also likely to assist the B800 → B850 RET at low temperatures. Clearly, delocalized exciton states in the LH2 complex are intimately related to its highly optimized design for efficient and robust RET dynamics. While this is an important step forward for the elucidation of the quantum dynamical effects, it is also true that further examination of proposed MC effects and other contributions need to continue. These include more thorough examination of the effects of the disorder and temperature, the role of coherence within B800,[122] and the back transfer from B850 to B800.[41,136] Considering that the interpretation of various spectroscopic information on LH2 is not far from being settled, a comprehensive theoretical effort accounting for all major experimental findings and development of a more advanced theoretical tool that allows large-scale calculation of open system quantum dynamics are required. Recent theoretical analysis[137] of single molecule spectroscopy and the development of PQME approach[96,109,110] for CRET are significant steps forward in this regard.

Photosynthetic Reaction Center

The LH2 complex from purple bacteria proved to be a prototypical system demonstrating clear MC effects in the RET process. In addition to the highly symmetric light-harvesting systems of purple bacteria, natural photosynthetic organisms utilize compact photosynthetic complexes with a great variety in structures and the arrangement of chromophores for efficient light-energy harvesting.[32] These photosynthetic systems, including antenna complexes and reaction centers (RCs), often exhibit clusters of strongly coupled chromophores and efficient energy transfer between them. As a result, MC effects should play important roles in many of these systems as in LH2.

For example, the RC of purple bacteria represents a typical photosynthetic system that requires a treatment based on the MC-FRET theory to explain its energy transfer properties. Figure 6 shows the linear absorption spectrum and arrangement of pigments in the RC from the purple bacterium *Rhodobacter (Rb.) sphaeroides*. This RC contains two bateriochorophylls (Bchl) called the special pair

 © 2012 John Wiley & Sons, Ltd.

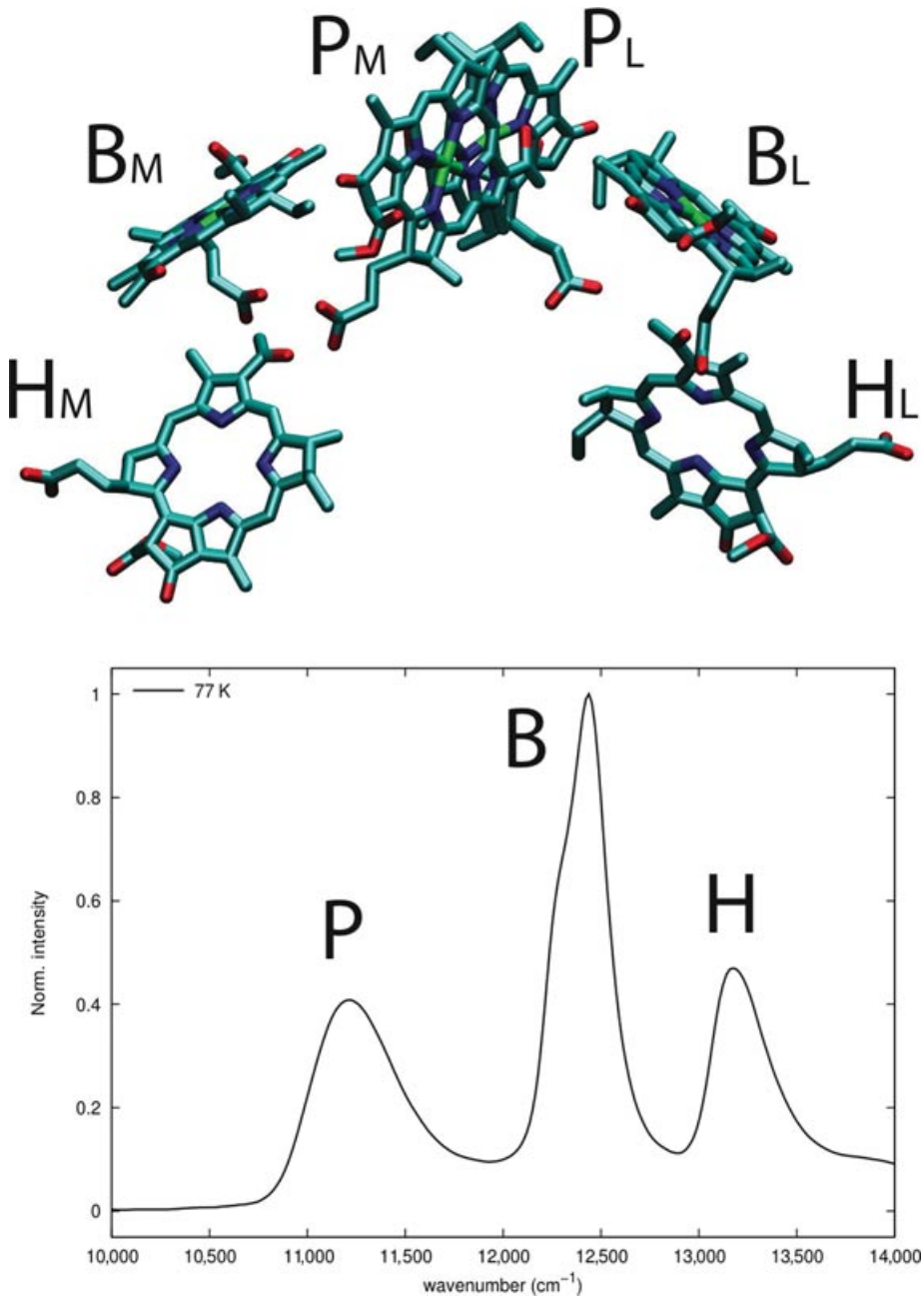

FIGURE 6 | Arrangement of bacteriochlorophylls (P_M, P_L, B_M, and B_L) and bacteriopheophytins (H_M and H_L) in the RC from the purple bacterium *Rb. sphaeroides*, and the experimental linear absorption spectrum measured at 77 K.

(P) in the center, an accessory Bchl flanking P on each side (B_L and B_M), and a bateriopheophytin (H_L and H_M) next to each B. Upon excitation of P, the RC quickly undergoes charge separation to convert solar energy into chemical potential with a quantum efficiency near 1 in about 3 ps at room temperature. In addition, as early as 1972, absorption measurements performed by Slooten have indicated that excitation energy transfer from H and B to P occurs in the RC of *Rb. sphaeroides* in the ultrafast timescale (H to B in about 100 fs and from B to P in about 150 fs) with very little temperature dependence.[138,139]

If the energy transfer has been dominated by the Förster mechanism, the modest spectral overlap between B and P at low temperatures and the significant spectral dependence on the temperature would predict very different RET behavior.[140,141] Theoretical calculations based on the FRET theory predicted a

 © 2012 John Wiley & Sons, Ltd.

time constant of ~ 3 ps, which is mainly attributable to the modest donor–acceptor spectral overlap.[140] This result fails to explain the ultrafast timescales of RET and has motivated numerous discussion concerning the mechanism of energy transfer within the RC.[140,142,143] The puzzle was not resolved until it was recognized that since the two chlorophylls in the special pair are coupled strongly, much like the B800 → B850 RET case mentioned above, it is necessary to consider energy transfer from B to a coherently delocalized P state.[92,141,144] In particular, a detailed study carried out by Jordanides et al. using an adaptation of the Förster theory with correct calculation of effective donor-acceptor couplings and their associated spectral overlaps demonstrated that the RET dynamics in the RC are described by a weak-coupling mechanism.[141] Again, the MC effect necessitates that a picture of RET between coherently delocalized states must be considered to describe experimental results.

The MC-FRET theory (in a slight different form) has also been applied to describe energy transfer from the peripheral chlorophyll connecting the antenna system to the six coupled core pigments of the RC of photosystem II.[145,146] This system also critically depends on the MC effects, and the energy transfer process was shown to be directly coupled to the energy trapping by primary charge separation in the PS II RC.[145] It seems that general coherence-assisting principles play important roles in many photosynthetic light-harvesting complexes. However, they have to be examined in more details in other photosynthetic complexes before any general conclusion is drawn. Interestingly, recent work by Schlau-Cohen et al. also indicates the importance of coherence in defining the pathways of energy flow in the major light-harvesting complex of higher plants.[147]

Artificial Organic Materials

RET in organic crystals, thin films, and aggregates is an area of significant current interest due to the potential application for organic optoelectronic and energy devices. Historically, this is the field where general theoretical frameworks were laid out for CRET and the effects of quantum coherence were scrutinized intensively.[6,30,121,148] An important issue that dominated the literature in the 1960s to 1980s is the temperature-dependent transition from coherent to incoherent mechanisms of the exciton mobility in molecular crystals. Most recently, coherence effects in two-dimensional (2D) excitons in oligoacene molecular crystals was considered by Emelianova et al.[149] These molecular crystals exhibit herringbone-like structure in which the molecules are more strongly coupled within the layers and only weakly coupled in the interlayer directions. As a result, the energy carriers are best described as intralayer delocalized 2D excitons that move along the interlayer direction. Emelianova et al. applied a generalization of the FRET theory to calculate the effective couplings between such 2D excitons. This approach results in the renormalization of couplings between interlayer 2D excitons that enhances the interlayer transfer rate significantly. The enhancement comes from many contributing channels involving optically dark exciton states and can explain experimental observation. This work confirms the significance of generalized theories such as MC-FRET as new guiding principles for the design of artificial energy materials.

Molecular aggregation has significant ramifications on the optical response of organic materials. It is well known that photoexcitations in organic aggregates can delocalize over several tens or even hundreds of molecules.[150,151] As revealed in the *Recent Theoretical Developments* section, simple FRET theory cannot account for the RET dynamics in these materials, and at least the MC effects should be considered. Scholes investigated such MC effect in a model system consisting of a single donor molecule and a 2D array of acceptor molecules.[65,152] This study demonstrated an interesting example of "super" transfer caused by large effective coupling between the donor and the set acceptor molecules that are coupled strongly among themselves and form superradiant exciton states. This is another example that RET dynamics in complex molecular assemblies can be significantly affected by physics that are not captured by the simple FRET theory. Clearly, although the theories described in the *Recent Theoretical Developments* section were motivated by RET dynamics in photosynthetic systems, their applications and potential to reveal new photophysics and design principles in artificial systems can be significant. A theoretical study in this direction just started,[153] and investigation of MC, inelastic, and coherence effects in the RET dynamics of pi-conjugated systems remains an important theoretical subject.

CONCLUSION AND OPEN ISSUES

Motivated by intriguing experimental results and theoretical developments, the RET dynamics of coherently delocalized excitons have become the subjects of intensive studies in recent years. In this work, we provided a cross section of such efforts related to our works, by reviewing theoretical developments and applications to biological and macromolecular

 © 2012 John Wiley & Sons, Ltd.

systems. In particular, the successful generalization of the FRET theory to include MC effects has deepened our understanding of the mechanisms of RET involving coupled molecular aggregates within the rate description. A key insight gained is that the basis of RET process must be reexamined carefully and that the choice of coherently delocalized states as the unit of energy transfer can provide a more accurate description. Given the heterogeneous nature of natural photosynthetic systems and macromolecular organic aggregates, the additional realism incorporated into the MC-FRET description should have broad applications.

We also reviewed recent advances in the understanding of energy transfer mechanisms in the LH2 complex of purple bacteria. In this complex, intradonor or intraacceptor quantum coherence clearly plays fundamental roles in spectral properties, energy tuning, and the energy flow dynamics. The new design principles revealed by application of MC-FRET to LH2 may have great implications for the design of artificial systems. Whether similar effects can be identified for inter donor–acceptor quantum coherence is an interesting subject to explore for more general arrangement of chromophores.

In the future, advances in ultrafast spectroscopic methods will continue to provide critical tests of new theoretical developments, and it is important to engage close interactions between experiments and theories to explore new frontiers of RET dynamics in complex molecular aggregates. A central issue in this research is the characterization and assessment of electronic quantum coherence. The newly developed PQME approach[96,109–113] for CRET as well as other approaches[102,154–156] will find great utility in answering this question.

There are a couple of important open issues to be addressed for more reliable description of the RET dynamics. The FRET and all the theories described in this work are based on the assumption that local field effect can be neglected. As noted by Knox and van Amerongen,[157] consideration of local field effects involve subtle issues that require careful treatment. Formulation at the level quantum electrodynamics formalism[158,159] may be necessary to address them. On the other hand, heterogeneity of local field effect was found to be significant and can play a role in high efficiency of energy flow in light-harvesting systems.[160] Similar effects may be found in other natural and synthetic systems as well.

Another key open issue is reliable specification and determination of the spectral density, which plays a fundamental role in the RET dynamics. Most spectral densities being used so far have been determined by fitting to spectroscopic data. While these may provide adequate description of relevant spectroscopic observables, they may not be sufficient to gain correct microscopic understanding of the effects of exciton–protein interactions and of the roles of the environments. Olbrich et al. recently investigated environmental effects on electronic transitions in the Fenna-Matthews-Olson photosynthetic complex using a combined molecular dynamics and quantum chemistry approach.[60,161] Further advances in this direction are needed to elucidate molecular level details critical for RET process.

NOTES

[a]The physical implication of this term is ambiguous and can be misleading because what is being transferred is not the fluorescence but the energy.

ACKNOWLEDGMENTS

The authors dedicate this work to the late Bob Silbey who has provided unabating inspiration and guidance throughout this research. SJ was supported by the U.S. National Science Foundation CAREER award (grant no. CHE-0846899), the Office of Basic Energy Sciences, Department of Energy (grant no. DE-SC0001393), and the Camille Dreyfus Teacher Scholar Award. YCC thanks the National Science Council, Taiwan (grant no. NSC 100-2113-M-002-004-MY2), National Taiwan University (grant no. 10R80912-5), and Center for Quantum Science and Engineering (subproject: 10R80914-1) for financial support.

REFERENCES

1. Davydov AS. *Theory of Molecular Excitons*. NewYork: Plenum Press; 1971.
2. Förster Th. In Sinanoglu, O., Ed., *Modern Quantum Chemistry*, Part III. New York: Academic Press; 1965.

 © 2012 John Wiley & Sons, Ltd.

3. Silbey R. Electronic-energy transfer in molecular-crystals. *Annu Rev Phys Chem* 1976, 27:203.
4. Rashba EI, Sturge MD, Eds. *Modern Problems in Condensed Matter Sciences: Vol. 2, Excitons*. Amsterdam, The Netherlands: North-Holland; 1982.
5. Reineker P, Haken H, Wolf HC, Eds. *Organic Molecular Aggregates*. Berlin: Springer-Verlag; 1983.
6. Kenkre VM, Reineker P. *Exciton Dynamics in Molecular Crystals and Aggregates*. Berlin: Springer; 1982.
7. Sundstrom V, Pullerits T, van Grondelle R. Photosynthetic light-harvesting: reconciling dynamics and structure of purple bacteria LH2 reveals function of photosynthetic unit. *J Phys Chem* B 1999, 103:2327.
8. Hu X, Ritz T, Damjanovic A, Autenrieth F, Schulten K. Photosynthetic apparatus of purple bacteria. *Quar Rev Biophys* 2002, 35:1.
9. Renger T, May V, and Kühn O. Ultrafast excitation energy transfer dynamics in photosynthetic pigment-protein complexes. *Phys Rep* 2001, 343:137.
10. Cogdell RJ, Gali A, and Köhler J. The architecture and function of the light-harvesting apparatus of purple bacteria: from single molecules to in vivo membranes. *Quart Rev Biophys* 2006, 39:227.
11. Heeger AJ. Semiconducting and metallic polymers: The fourth generation of polymeric materials. *Rev Mod Phys* 2000, 73:681.
12. Bittner ER. Exciton dynamics—simplifying organic complexity. *Nature Phys* 2006, 2:591.
13. Gaab KM, Bardeen CJ. Wavelength and temperature dependence of the femtosecond pump-probe anisotropies in the conjugated polymer MEH-PPV: implications for energy transfer dynamics. *J Phys Chem* B 2004, 108:4619–4626.
14. Lim SH, Bjorklund TG, Gaab KM, Bardeen CJ. The role of long-lived dark states in the photoluminescence dynamics of phenylene vinylene conjugated polymers. *J Chem Phys* 2002, 117:454.
15. Beljonne D, Hennebicq E, Daniel C, Herz LM, Silva C, Scholes GD, Hoeben FJM, Jonkheijm P, Schenning APHJ, Meskers SCJ, et al. Excitation migration along oligophenylenevinylene-based chiral stacks: delocalization effects on transport dynamics. *J Phys Chem* B 2005, 109:10594.
16. Collini E, Scholes GD. Coherent intrachain energy migration in a conjugated polymer at room temperature. *Science* 2009, 323:369–373.
17. Spano FC. Excitons in conjugated oligomer aggregates, films, and crystals. *Annu Rev Phys Chem* 2006, 57:217.
18. Cao J, Silbey RJ. Optimization of exciton trapping in energy transfer processes. *J Phys Chem* A 2009, 113:13825–13838.
19. Frenkel J. On the transformation of light into heat in solids. I. *Phys Rev* 1931, 37:17–44.
20. Förster Th. Intermolecular energy migration and fluorescence. *Ann Phys*1948, 6:55.
21. Dexter DL. A theory of sensitized luminescence in solids. *J Chem Phys* 1953, 21:836–850.
22. Gochanour CR, Andersen C, Fayer MD. Electronic excited state transport in solution. *J Chem Phys* 1979, 70:4254–4271.
23. Haan SW, Zwanzig R. Förster migration of electronic excitation between randomly distributed molecules. *J Chem Phys* 1978, 68:1879–1883.
24. Godzik K, Jortner J. Electronic energy transfer in impurity band. *Chem Phys* 1979, 38:227–237.
25. Huber DL. Fluorescence in the presence of traps. *Phys Rev* B 1979, 20:2307.
26. Blumen A, Klafter J, Silbey R. Energy transfer in disordered media. *J Chem Phys* 1980, 72:5320–5332.
27. Loring RF, Andersen HC, Fayer MD. Electronic excited state transport and trapping in solution. *J Chem Phys* 1982, 76:2015–2027.
28. Fedorenko SG, Burshtein AI. Binary theory of impurity quenching accelerated by resonant excitation migration in a disordered system. *Chem Phys* 1988, 128:185.
29. Jang S, Shin KJ, Lee S. Effects of excitation migration and translational diffusion in luminescence quenching dynamics. *J Chem Phys* 1995, 102:815.
30. Grover M, Silbey R. Exciton migration in molecular crystals. *J Chem Phys* 1971, 54:4843.
31. Kenkre VM, Knox RS. Generalized master equation theory of excitation transfer. *Phys Rev* B 1974, 9:5279.
32. Cogdell RJ, Gardiner AT, Hashimoto H, Brotosudarmo THP. A comparative look at the first few milliseconds of the light reactions of photosynthesis. *Photochem Photobiol Sci* 2008, 7:1150–1158.
33. Kopelman R, Shortreed M, Shi ZY, Tan W, Xu Z, Moore JS, Bar-Haim A, Klafter J. Spectroscopic evidence for excitonic localization in fractal antenna supermolecules. *Phys Rev Lett* 1997, 78:1239.
34. Hofkens J, Maus M, Gensch T, Vosch T, Cotlet M, Köhn F, Hermann A, Müllen K, Schryver FCD. Probing photophysical processes in individual multichromophoric dendrimers by single molecule spectroscopy. *J Am Chem Soc* 2000, 122:9278.
35. Ranasinghe MI, Wang Y, Goodson T III. Excitation energy transfer in branched dendritic macromolecules at low (4 K) temperatures. *J Am Chem Soc* 2003, 125:5258–5259.
36. Ahn TA, Nantalaksakul A, Dasari RR, Al Kaysi RO, Müller AM, Thayumanavan S, Bardeen CJ. Energy and charge transfer dynamics in fully decorated benzyl ether dendrimers and their disubstituted analogues. *J Phys Chem* B 2006, 110:24331.

 © 2012 John Wiley & Sons, Ltd.

37. Peng Z, Melinger J, Kleiman V. Light harvesting unsymmetrical conjugated dendrimers as photosynthetic mimics. *Photosyn Res* 2006, 87:115.
38. Kleiman VD, Melinger JS, McMorrow D. Ultrafast dynamics of electronic excitations in a light harvesting phenylactylene dendrimer. *J Phys Chem* B 2001, 105:5595.
39. Varnavski OP, Ostrowski J, Sukhomlinova L, Twieg RJ, Bazan GC, Goodson T III. Coherent effects in energy transport in model dendritic structures investigated by ultrafast fluorescence anisotropy spectroscopy. *J Am Chem Soc* 2002, 124:1736–1743.
40. Kim D, Osuka A. Directly linked prophyrin arrays with tunable excitonic interactions. *Acc Chem Res* 2004, 37:735.
41. Yang M, Agarwal R, Fleming GR. The mechanism of energy transfer in the antenna of photosynthetic purple bacteria. *J Photochem Photobiol A: Chem* 2001, 142:107.
42. Yang M, Damjanović A, Vaswani HM, and Fleming GR. Energy transfer in photosystem I of cyanobacteria *Synechococcus elongatus*: model study with structure based semi-empirical Hamiltonian and experimental spectral density. *Biophys J* 2003, 85:140.
43. Jang S, Newton MD, Silbey RJ. Multichromophoric Förster resonance energy transfer. *Phys Rev Lett* 2004, 92:218301.
44. Jang S, Newton MD, Silbey RJ. Multichromophoric Förster resonance energy transfer from B800 to B850 in the light harvesting complex 2: evidence for subtle energetic optimization by purple bacteria. *J Phys Chem* B 2007, 111:6807.
45. Brédas JL, Norton JE, Cornil J, Coropceanu V. Molecular understanding of organic solar cells: The Challenges. *Acc Chem Res* 2009, 42:1691–1699.
46. Chasteen SV, Sholin V, Carter SA, Rumbles G. Towards optimization of device performance in conjugated polymer photovoltaics: charge generation, transfer and transport in poly(*p*-phenylene-vinylene) polymer heterojunctions. *Solar Energy Mater Solar Cells* 2008, 92:651.
47. Bolinger JC, Traub MC, Adachi T, Barbara PF. Ultralong-range polaron-induced quenching of excitons in isolated conjugated polymers. *Science* 2011, 331:565–567.
48. Bardeen C. Exciton quenching and migration in single conjugated polymers. *Science* 2011, 331:544.
49. Mukamel S, *Principles of Nonlinear Spectroscopy*. New York: Oxford University Press; 1995.
50. Jonas DM. Two-dimensional femtosecond spectroscopy. *Annu Rev Phys Chem* 2003, 54:425.
51. Cho M, Vaswani HM, Brixner T, Stenger J, Fleming GR. Exciton analysis in 2D electronic spectroscopy. *J Phys Chem* B 2005, 109:10542.
52. Cho M. Coherent two-dimensional optical spectroscopy. *Chem Rev* 2008, 108:1331.
53. Engel GS, Calhoun TR, Read EL, Ahn TK, Mancal T, Cheng YC, Blankenship RE, Fleming GR. Evidence for wavelike energy transfer through quantum coherence in photosynthetic systems. Nature 2007, 446:782–786.
54. Collini E, Wong CY, Wilk KE, Curmi PMG, Brumer P, Scholes GD. Coherently wired light-harvesting in photosynthetic marine algae at ambient temperature. Nature 2010, 463:644–647.
55. Panitchayangkoon G, Hayes D, Fransted KA, Caram JR, Harel E, Wen J, Blankenship RE, Engel GS. Long-lived quantum coherence in photosynthetic complexes at physiological temperature. *Proc Natl Acad Sci USA* 2010, 107:12766.
56. Schlau-Cohen GS, Ishizaki A, Fleming GR. Two-dimensional electronic spectroscopy and photosynthesis: fundamentals and applications to photosynthetic light-harvesting. *Chem Phys* 2011, 386:1–22.
57. Palmieri B, Abramvicius D, Mukamel S. Interplay of slow bath fluctuations and energy transfer in 2D spectroscopy of the FMO light-harvesting complex: benchmarking of simulation protocols *Phys Chem Chem Phys* 2010, 12:108–114.
58. Sharp LZ, Egorova D, Domcke W. Efficient and accurate simulations of two-dimensional electronic photon-echo signals: illustration for a simple model of the Fenna–Matthews–Olson complex. *J Chem Phys* 2010, 132:014501.
59. Abramvicius D, Mukamel S. Quantum oscillatory exciton migration in photosynthetic reaction centers. *J Chem Phys* 2010, 133:064510.
60. Olbrich C, Jansen TLC, Liebers J, Aghtar M, Strümpfer J, Schulten K, Knoester J, Kleinekathöfer U. From atomistic modeling to excitation transfer and two-dimensional spectra of the FMO light-harvesting complex. *J Phys Chem* B 2011, 115:8609–8621.
61. Chen L, Zheng R, Jing Y, Shi Q. Simulation of the two-dimensional electronic spectra of the Fenna–Matthews–Olson complex using the hierarchical equations of motion method. *J Chem Phys* 2011, 134:194508.
62. Agranovich VM, Galanin MD, *Modern Problems in Condensed Matter Sciences: Vol.3, Electronic Excitation Energy Transfer in Condensed Matter*. Amsterdam: North-Holland; 1982.
63. Birks JB, ed. *Excited States of Biological Molecules*. London: John Wiley & Sons; 1976.
64. Andrews DL, Demidov AA, eds. *Resonance Energy Transfer*. Chichester, UK: John Wiley & Sons; 1999.
65. Scholes GD. Long range resonance energy transfer in molecular systems. *Annu Rev Phys Chem* 2003, 54:57.
66. Ha T, Enderle T, Ogletree DF, Chemla DS, Selvin PR, Weiss S. Probing the interaction between two single molecules: Fluorescence resonance energy transfer

 © 2012 John Wiley & Sons, Ltd.

between a single donor and a single acceptor. *Proc Natl Acad Sci* 1996, 93:6264.

67. Lipman EA, Schuler B, Bakajin O, Eaton WA. Single-molecule measurement of protein folding kinetics. *Science* 2003, 301:1233.
68. Thompson AL, Gaab KM, Xu J, Bardeen CJ, Martínez TJ. Variable electronic coupling in phenylacetylene dendrimers: the role of Förster, Dexter, and charge-transfer interactions. *J Phys Chem* A 2004, 108:671.
69. Wong KF, Bagchi B, Rossky PJ. Distance and orientational dependence of excitation transfer rates in conjugated systems: beyond the Förster theory. *J Phys Chem* A 2004, 108:5752.
70. Russo V, Curutchet C, Mennucci B. Towards a molecular scale interpretation of excitation energy transfer in solvated bichromophoric systems. II. The through-bond contribution. *J Phys Chem* B 2007, 111:853.
71. Nguyen TQ, Wu J, Doan V, Schwartz BJ, Tolbert SH. Control of energy transfer in oriented conjugated polymer-mesoporous silica composites. *Science* 2000, 288:652.
72. Hsiao JS, Krueger B, Wagner W, Johonson TE, Delaney JK, Mazuerall D, Fleming GR, Lindsey JS, Bocian DF, Donohoe RJ. Soluble synthetic multiporphyrin arrays. 2. Phtodynamics of energy-transfer processes. *J Am Chem Soc* 1996, 118:11181–11193.
73. Yang SI, Lammi RK, Seth J, Riggs JA, Arai T, Kim D, Bocian D, Holten D, Lindsey J. Excited-state energy transfer and ground-state hole/electron hopping in *p*-phenylene-linked porphyrin dimers. *J Phys Chem* B 1998, 102:9426.
74. Serin JM, Brousmiche DW, Fréchet JMJ. Cascade energy transfer in a conformationally mobile multichromophoric dendrimer. *Chem Commun* 2002, 22:2605.
75. Gronheid R, Hofkens J, Kohn F, Weil T, Reuther E, Mullen K, Schryver FCD. Intramolecular Förster energy transfer in a dendritic system at the single molecule level. *J Am Chem Soc* 2002, 124:2418.
76. Aratani N, Cho HS, Ahn TK, Cho S, Kim D, Sumi H, Osuka A. Efficient excitation energy transfer in long meso-meso linked Zn(II) porphyrinarrays bearing a 5,15-bisphenylethynylated Zn(II) porphyrin acceptor . *J Am Chem Soc* 2003, 125:9668.
77. Hindin E, Forties RA, Loewe RS, Ambroise A, Kirmaier C, Bocian D, Lindsey JS, Holten D, Knox RS. Excited-state energy flow in covalently linked multiporphyrin arrays: the essential contribution of energy transfer between nonadjacent chromophores. *J Phys Chem* B 2004, 108:12821.
78. Fan C, Wang S, Hong JW, Bazan GC, Plaxco KW, Heeger AJ. Beyond superquenching: hyper-efficient energy transfer from conjugated polymers to gold nanoparticles. *Proc Natl Acad Sci* 2003, 100:6297.
79. Chen CH, Liu KY, Sudhakar S, Lim TS, Fann W, Hsu CP, Luh TY. Efficient light harvesting and energy transfer in organic-inorganic hybrid multichromophoric materials. *J Phys Chem* B 2005, 109:17887.
80. Schlosser M, Lochbrunner S. Exciton migration by ultrafast Förster transfer in highly doped matrices. *J Phys Chem* B 2006, 110:6001.
81. Praveen VK, George SJ, Varghese R, Vijayakumar C, Ajayaghosh A. Self-assembled π-nanotapes as donor scaffolds for selective and thermally gated fluorescence resonance energy transfer (FRET). *J Am Chem Soc* 2002, 124:4436.
82. Stryer L, Haugland RP. Energy transfer: a spectroscopic ruler. *Proc Natl Acad Sci USA* 1967, 58:719.
83. Haugland RP, Yguerabide J, Stryer L. Dependence of the kinetics of singlet-singlet energy transfer on spectral overlap. *Proc Natl Acad Sci USA* 1969, 63:23.
84. Selvin PR. The renaissance of fluorescence resonance energy transfer. *Nature Struct Biol* 2000, 7:730.
85. Hillisch A, Lorenz M, Diekmann S. Recent advances in FRET: distance determination in protein-DNA complexes. *Curr Opin Struct Biol* 2001, 11:201.
86. Heyduk T. Measuring protein conformational changes by FRET/LRET. *Curr Opin Biotechnol* 2002, 13:292.
87. Koushik SV, Chen H, Thaler C, Puhl HL III, Vogel SS. Cerulean, Venus, and Venus (Y67C) FRET reference standards *Biophys J* 2006, 91:L99–L101.
88. Jang S. Generalization of the Förster resonance energy transfer theory for quantum mechanical modulation of the donor-acceptor coupling. *J Chem Phys* 2007, 127:174710.
89. Soules TF, Duke CB. Resonant energy transfer between localized electronic states in a crystal. *Phys Rev* B 1971, 3:262.
90. Jang S, Jung YJ, Silbey RJ. Nonequilibrium generalization of Förster–Dexter theory foor excitation energy transfer. *Chem Phys* 2002, 275:319–332.
91. Hennebicq E, Beljonne D, Curutchet C, Scholes GD, Silbey RJ. Shared-mode resonant energy transfer in the weak coupling regime. *J Chem Phys* 2009, 130:214505.
92. Sumi H. Theory of rates of excitation-energy transfer between molecular aggregates through distributed transition dipoles with application to the antenna system in bacterial photosynthesis. *J Phys Chem* B 1999, 103:252.
93. Lippitz M, Hübner CH, Christ T, Eichner H, Bordat P, Herrmann A, Müllen K, Basché T. Coherent electronic coupling versus localization in individual molecular dimers. *Phys Rev Lett* 2004, 92:103001.
94. Yamazaki I, Akimoto S, Yamazaki T, Sato S, Sakata Y. Oscillatory excitation transfer in dithiaanthracenophene: Quantum beat in a coherent photochemical process in solution. *J Phys Chem* A 2002, 106:2122–2128.
95. Collini E, Scholes GD. Electronic and vibrational coherences in resonance energy transfer along

 © 2012 John Wiley & Sons, Ltd.

MEH-PPV chains at room temperature. *J Phys Chem* A 2009, 113:4223.

96. Jang S, Cheng YC, Reichman DR, Eaves JD. Theory of coherent resonance energy transfer. *J Chem Phys* 2008, 129:101104.
97. May V. Higher-order processes of excitation energy transfer in supramolecular complexes: Liouville space analysis of bridge molecule mediated transfer and direct photon exchange. *J Chem Phys* 2008, 129:114109.
98. Gilmore JB, McKenzie RH. Quantum dynamics of electronic excitations in biomolecular chromophores: role of the protein environment and solvent. *J Phys Chem* A 2008, 112:2162.
99. Yu ZG, Berding MA, Wang H. Spatially correlated fluctuations and coherence dynamics in photosynthesis. *Phys Rev* E 2008, 78:050902.
100. Palmieri B, Abramvicius D, Mukamel S. Lindblad equations for strongly coupled populations and coherences in photosynthetic complexes. *J Chem Phys* 2009, 130:204512.
101. Ishizaki A, Fleming GR. On the adequacy of the Redfield equation and related approaches to the study of quantum dynamics in electronic energy transfer. *J Chem Phys* 2009, 130:234110.
102. Ishizaki A, Fleming GR. Unified treatment of quantum coherent and incoherent hopping dynamics in electronic energy transfer: reduced hierarchy equation approach. *J Chem Phys* 2009, 130:234111.
103. Mohseni M, Rebentrost P, Loyd S, Aspuru-Guzik A. Environment-assisted quantum walks in photosynthetic energy transfer. *J Chem Phys* 2008, 129:174106.
104. Olaya-Castro A, Lee CF, Olsen FF, Johnson NF. Efficiency of energy transfer in a light-harvesting system under quantum coherence. *Phys Rev* B 2008, 78:085115.
105. Förster T. Transfer mechanisms of electronic excitation. *Discuss Faraday Soc* 1959, 27:7.
106. Jean JM, Fleming GR. Competition between energy and phase relaxation in electronic curve crossing processes. *J Chem Phys* 1995, 103:2092.
107. Wynne K, Hochstrasser RM. Anisotropy as an ultrafast probe of electronic coherence in degenerate systems exhibiting raman-scattering, fluorescence, transient absorption, and chemical-reacations. *J Raman Spectrosc* 1995, 26:561–569.
108. Yang M, Fleming GR. Influence of phonons on excitation transfer dynamics: comparison of the Redfield, Förster, and modified Redfield equations. *Chem Phys* 2002, 275:355.
109. Jang S. Theory of coherent resonance energy transfer for coherent initial condition. *J Chem Phys* 2009, 131:164101.
110. Jang S. Theory of multichromophoric coherent resonance energy transfer: a polaronic quantum master equation approach. *J Chem Phys* 2011, 135: 034105.
111. Nazir A. Correlation-dependent coherent to incoherent transitions in resonant energy transfer dynamics. *Phys Rev Lett* 2009, 103:146404.
112. McCutcheon DPS, Nazir A. Consistent treatment of coherent and incoherent energy transfer dynamics using a variational master equation. *J Chem Phys* 2011, 135:114501.
113. Kolli A, Nazir A, Olaya-Castro A. Electronic excitation dynamics in multichromophoric systems described via polaron-representation master equation. *J Chem Phys* 2011, 135:154112.
114. Holstein T. Studies of polaron motion: Part I. The molecular-crystal model. Ann Phys 1959, 8:325-342; Studies of polaron motion: Part II. The "small" polaron. *J Chem Phys* 1959, 8:343–389.
115. Silbey R, Harris RA. On the calculation of transfer rates between impurity states in solids. *J Chem Phys* 1984, 80:2615.
116. Harris RA, Silbey R.Variational calculation of the tunneling system interacting with a heat bath. II. Dynamics of an asymmetric tunneling system. *J Chem Phys* 1985, 83:1069.
117. Suárez A, Silbey R. Hydrogen tunneling in condensed media. *J Chem Phys* 1991, 94:4809.
118. Rackovsky S, Silbey R. Electronic energy transfer in impure solids I. Two molecules embedded in a lattice. *Mol Phys* 1973, 25:61.
119. Jackson B, Silbey R. On the calculation of transfer rates between impurity states in solids. *J Chem Phys* 1983, 78:4193.
120. Cheng YC, Silbey RJ. A unified theory for charge-carrier transport in organic crystals. *J Chem Phys* 2008, 128:114713.
121. Yarkony DR, Silbey RJ. Comments on exciton phonon coupling —temperature-dependence. *J Chem Phys* 1976, 65:1042–1052.
122. Cheng YC, Silbey RJ. Coherence in the B800 ring of purple bacteria LH2. *Phys Rev Lett* 2006, 96:028103.
123. McDermott G, Prince SM, Freer AA, Hawthornthwaite-Lawless AM, Paplz MZ, Cogdell RJ, Issacs NW. Crystal structure of an integral membrane light-harvesting complex from photosynthetic bacteria. *Nature* 1995, 374:517.
124. Jang S, Silbey RJ. Single complex line shapes of the B850 band of LH2. *J Chem Phys* 2003, 118:9324.
125. Jang S, Dempster SE, Silbey RJ. Characterization of the static disorder in the B850 band of LH2. *J Phys Chem* B 2001, 105:6655.
126. Renger T, Marcus RA. On the relation of protein dynamics and exciton relaxation in pigment-protein complexes: an estimate of the spectral density and a theory for the calculation of optical spectra. *J Chem Phys* 2002, 116:9997.

 © 2012 John Wiley & Sons, Ltd.

127. Pullerits T, Hess S, Herek JL, Sundström V. Temperature dependence of excitation transfer in LH2 of *Rhodobacter sphaeroides*. *J Phys Chem* B 1997, 101:10560.
128. Scherz A, Parson WW. Exciton interactions in dimers of bacteriochlorophyll and related molecules. *Biochim Biophys Acta* 1984, 766:666–678.
129. Monshouwer R, Abrahamsson M, van Mourik F, van Grondelle R. J. Superradiance and exciton delocalization in bacterial photosynthetic light-harvesting systems. *Phys Chem* B 1997, 101:7241–7248.
130. Mukai K, Abe S, Sumi H. Theory of rapid excitation-energy transfer from B800 to optically-forbidden exciton states of B850 in the antenna system LH2 of photosynthetic purple bacteria. *J Phys Chem* B 1999, 103:6096.
131. Scholes GD, Fleming GR. On the mechanism of light harvesting in photosynthetic purple bacteria: B800 to B850 energy transfer. *J Phys Chem* B 2000, 104:1854.
132. Salverda JM, van Mourik F, van der Zwan G, van Grondelle R. Energy transfer in the B800 rings of the peripheral bacterial light-harvesting complexes of *Rhodopseudomonas acidophila* and *Rhodospirillum molischianum* studied with photon echo techniques. *J Phys Chem* B 2000, 104:11395.
133. Agarwal R, Yang M, Xu QH, Fleming GR. Three pulse photon echo peak shift study of the B800 band of the LH2 complex of Rps. acidophila at room temperature: A coupled master equation and nonlinear optical response function approach. J. Phys. Chem. B 2001, 105:1887.
134. Krueger BP, Scholes GD, Fleming GR. Calculation of couplings and energy-transfer pathways between the pigments of LH2 by the *ab initio* transition density cube method. *J Phys Chem* B 1998, 102:5378–5386.
135. Scholes GD, Cogdell IRGRJ, Fleming GR. Ab initio molecular orbital calculations of electronic couplings in the LH2 bacterial light-harvesting complex of rps-acidophila. *J Phys Chem* B 1999, 103:2543–2553.
136. Kimura A, Kakitani T. Theoretical analysis of the energy gap dependence of the reconstituted B800 → B850 excitation energy transfer rate in bacterial LH2 complexes. *J Phys Chem* B 2003, 107:7932–7939.
137. Jang S, Silbey RJ, Kunz R, Hofmann C, Köhler J. Is there elliptic distortion in the light harvesting complex 2 of purple bacteria? *J Phys Chem* B 2011, 115:, 12947.
138. Vos M, Breton J, Martin MJ. Electronic energy transfer within the hexamer cofactor system of bacterial reaction centers. *J Phys Chem* B 1997, 101:9820–9832.
139. Stanley R, King B, Boxer S. Excited state energy transfer pathways in photosynthetic reaction centers .1. structural symmetry effects. *J Phys Chem* 1996, 100:12052–12059.
140. Jean J, Chan CK, Fleming GR. Electronic-energy transfer in photosynthetic bacterial reaction centers. *Israel J Chem* 1988, 28:169–175.
141. Jordanides XJ, Scholes GD, Fleming GR. The mechanism of energy transfer in the bacterial photosynthetic reaction center. *J Phys Chem* B 2001, 105:1652–1669.
142. King BA, Stanley R, Boxer S. Excited state energy transfer pathways in photosynthetic reaction centers .2. heterodimer special pair. *J Phys Chem* B 1997, 101:3644–3648.
143. Lin S, Taguchi A, Woodbury N. Excitation wavelength dependence of energy transfer and charge separation in reaction centers from rhodobacter sphaeroides: Evidence for adiabatic electron transfer. *J Phys Chem* B 1996, 100:17067–17078.
144. Scholes GD, Jordanides XJ, Fleming GR. Adapting the Förster theory of energy transfer for modeling dynamics in aggregated molecular assemblies. *J Phys Chem* B 2001, 105:1640.
145. Raszewaski G, Renger T. Light harvesting in photosystem II core complexes is limited by the transfer to the trap: Can the core complex turn into a photoprotective mode? *J Am Chem Soc* 2008, 130:4431–4446.
146. Raszewaski G, Renger T. Theory of optical spectra of photosystem ii reaction centers: location of the triplet state and the identity of the primary electron donor. *Biophys J* 2005, 88:986–998.
147. Schlau-Cohen GS, Calhoun TR, Ginsberg NS, Read EL, Ballottari M, Bassi R, van Grondelle R, Fleming GR. Pathways of energy flow in lhcii from two-dimensional electronic spectroscopy. *J Phys Chem* B 2009, 113:15352–15363.
148. Munn R, Silbey RJ. Remarks on exciton - phonon coupling and exciton transport. *Mol Cryst Liq Cryst* 1980, 57:131.
149. Emelianova EV, Athanasopoulos S, Silbey RJ, Beljone D. 2d excitons as primary energy carriers in organic crystals: The case of oligoacenes. *Phys Rev Lett* 2010, 104:206405.
150. Kobayashi, T., ed. *J-Aggregates*. Singapore: World Scientific; 1996.
151. Kasha M. Energy transfer mechanisms and molecular exciton model for molecular aggregates. *Radiat Res* 1963, 20:55.
152. Scholes GD. Designing light-harvesting antenna systems based on superradiant molecular aggregates. *Chem Phys* 2002, 275:373–386.
153. Yang L, Caprasecca S, Mennucci B, Jang S. Theoretical investigation of the mechanism and dynamics of intramolecular coherent resonance energy transfer in soft molecules: A case study of dithia-anthracenophane. *J Am Chem Soc* 2010, 132:16911–16921.
154. Huo P, Coker DF. Iterative linearized density matrix propagation for modeling coherent excitation energy

 © 2012 John Wiley & Sons, Ltd.

transfer in photosynthetic light harvesting. *J Chem Phys* 2010, 133:184108.

155. Zhu J, Kais S, Rebentrost P, Aspuru-Guzik A. Modified scaled hierarchical equation of motion approach for the study of quantum coherence in photosynthetic complexes. *J Phys Chem* B 2011, 115:1531–1537.
156. Strümpfer J, Schulten K. The effect of correlated bath fluctuations on exciton transfer. *J Chem Phys* 2011, 134:095102.
157. Knox RS, van Amerongen H. Refractive index dependence of the Förster resonance excitation transfer rate. *J Phys Chem* B 2002, 106:5289–5293.
158. Juzeliūnas G, Andrews DL. Quantum electrodynamics of resonant energy transfer in condensed matter. *Phys Rev* B 1994, 49: 8751.
159. Craig DP, Thirunamachandran T. *Molecular Quantum Electrodynamics: An Introduction to Radiation-Molecule Interactions*. London: Academic Press; 1984.
160. Curutchet C, Kongsted J, Muñoz-Losa A, H Hossein-Nejad GDS, Mennucci B. Photosynthetic light-harvesting is tuned by the heterogeneous polarizable environment of the protein. *J Am Chem Soc* 2011, 133:3078.
161. Olbrich C, Strümpfer J, Schulten K, Knoester J, Kleinekathöfer U. Theory and simulation of the environmental effects on fmo electronic transitions. *J Phys Chem Lett* 2011, 2:1771–1776.

 © 2012 John Wiley & Sons, Ltd.